

MARTI-MARS²: Scaling Multi-Agent Self-Search via Reinforcement Learning for Code Generation

Shijie Wang^{1*}, Pengfei Li^{3*}, Yikun Fu^{1,4*}, Kaifeng Liu³, Fangyuan Li³, Yang Liu⁵, Xiaowei Sun^{1,6}, Zonglin Li¹, Siyao Zhao⁵, Jian Zhao², Kai Tian^{2,9}, Dong Li³, Junqi Gao³, Yutong Zhang⁷, Yiqun Chen⁸, Yuqiang Li¹, Zoe Li¹⁰, Weinan Zhang³, Peng Ye¹, Shuyue Hu¹, Lei Bai¹, Bowen Zhou^{1,2}, Kaiyan Zhang^{2,9}, Biqing Qi¹^{✉,†}

¹Shanghai AI Laboratory, ²Tsinghua University, ³Harbin Institute of Technology, ⁴Shanghai Jiao Tong University, ⁵Institute of Automation, ⁶Fudan University, ⁷High School Affiliated to Fudan University, ⁸Renmin University of China, ⁹Frontis.AI, ¹⁰University of Washington

*Equal contributions, [✉]Project leaders, ^{✉,†}Corresponding authors

Correspondence: qibiqing@pjlab.org.cn, zhang-ky22@mails.tsinghua.edu.cn

Github: <https://github.com/TsinghuaC3I/MARTI>

Abstract | While the complex reasoning capability of Large Language Models (LLMs) has attracted significant attention, single-agent systems often encounter inherent performance ceilings in complex tasks such as code generation. To transcend these boundaries, multi-agent collaboration offers a promising avenue. However, existing frameworks typically rely on prompt-based test-time interactions or multi-role configurations trained with homogeneous parameters, which significantly limit the scope of error correction capabilities and strategic diversity. In this paper, we propose a Multi-Agent Reinforced Training and Inference Framework with Self-Search Scaling (MARTI-MARS²), which integrates policy learning with multi-agent tree search by formulating the multi-agent collaborative exploration process as a dynamic and learnable environment. Specifically, by allowing agents to iteratively explore and refine within the environment, the framework facilitates a evolution from parameter-sharing homogeneous multi-role training to heterogeneous multi-agent training, thereby breaking through the capability limits of single-agent. Complementing the training paradigms, we introduce an efficient inference strategy MARTI-MARS²-T+ to fully exploit the scaling potential of multi-agent collaboration at test time. We conduct extensive experiments across varied model scales (8B, 14B, and 32B) on challenging code generation benchmark, which serves as a proxy for complex reasoning tasks. Notably, utilizing two collaborating 32B models, MARTI-MARS² achieves a performance of 77.7%, outperforming strong baselines like GPT-5.1. Furthermore, MARTI-MARS² reveals a novel scaling law from multi-agent perspective: **shifting from single-agent to homogeneous multi-role and ultimately to heterogeneous multi-agent paradigms progressively yields higher RL performance ceilings, robust TTS capabilities, and greater policy diversity, suggesting that policy diversity is a critical dimension for scaling intelligence via multi-agent reinforcement learning.**

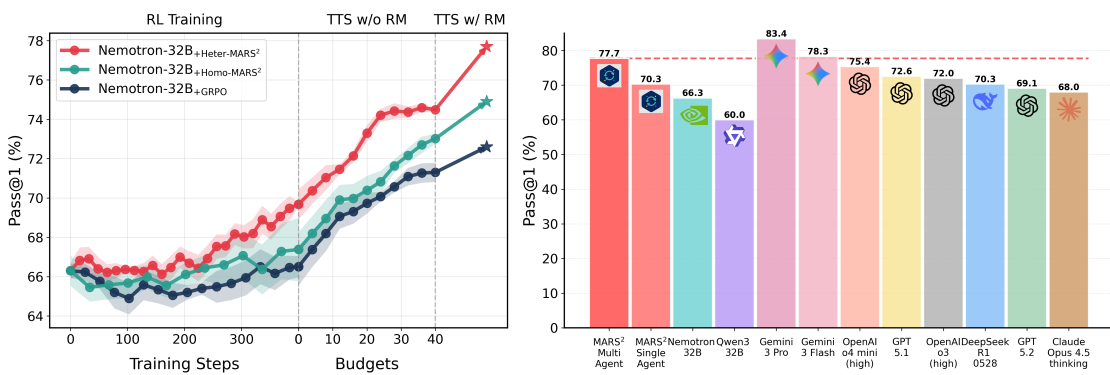


Figure 1: Multi-agent scaling laws and performance of MARTI-MARS². The left panel shows the scaling advantages in Nemotron-32B of the homogeneous multi-role method (Homo-MARS²) and heterogeneous multi-agent (Nemotron-32B and Qwen3-32B) method (Heter-MARS²) over single-agent (GRPO). The right panel compares the performance of MARTI-MARS² against leading open-source and closed-source LLMs.

Contents

1	Introduction	3
2	Method	4
2.1	Overview	4
2.2	The training paradigm of MARS ²	5
2.2.1	Multi-Agent Instantiation	5
2.2.2	Data Collection and Advantage Calculation	5
2.2.3	Data dispatching and Dynamic Training	6
2.2.4	The optimization objective of MARS ²	6
2.3	Test Time Scaling of MARS ²	7
2.3.1	Multi-Agent Refinement-based tree search	7
2.3.2	Reward Model of MARS ² -T+	8
3	Experiments	9
3.1	Experimental Setup	9
3.2	Results of Homo-MARS ²	10
3.3	Results of Heter-MARS ²	12
3.4	Results of MARS ² -T+	14
4	Diversity Analysis of MARS²	18
4.1	Diversity Metrics	18
4.2	Diversity Evaluation	20
5	Preliminary	22
5.1	GRPO	22
5.2	AB-MCTS	23
6	Related Works	24
6.1	Reinforcement Learning	24
6.1.1	Reinforcement Learning for LLM	24
6.1.2	Multi-Agent Reinforcement Learning	24
6.2	Test-Time Scaling	24
6.2.1	Single-Agent	24
6.2.2	Multi-Agent	25
7	Conclusion	25
8	Acknowledgements	25

1 Introduction

As the complex reasoning capability of Large Language Models (LLMs) emerges as a primary focus of contemporary research, significant progress has been achieved by optimizing robust chain-of-thought during post-training phase [39, 53, 16, 49] and by guiding efficient external search during test-time scaling phase [22, 35, 42, 66, 62]. Nevertheless, constrained by the inherent reasoning bounds of the base model’s pre-training, single agents often encounter performance ceilings in complex tasks such as code generation [71, 12]. To break this barrier, initial attempts aim to scale inference computation based on multi-agent systems, such as AutoGen [56] and MetaGPT [18]. However, these frameworks rely heavily on the models’ instruction-following capabilities and the pre-defined multi-agent workflow [44]. Therefore, recent research (e.g., Kimi K2.5 [41], Chain-of-Agents [28], and AT-GRPO [72]) have shifted from prompt-based test-time interaction to training LLMs for collaboration [37, 7, 8, 9], positing that coordination is an intrinsic capability to be optimized prior to inference. However, most existing multi-agent collaboration frameworks remain constrained to homogeneous multi-role settings, where agents share identical base models or parameters. Such homogeneity inherently limits the diversity of reasoning pathways, thereby capping the potential of heterogeneous agents to offer complementary perspectives and robust error correction mechanisms.

To further exploit the capabilities of heterogeneous systems, researchers design more general multi-agent training frameworks. MARFT [32] formulates multi-agent collaboration as a sequential decision-making problem to address the challenges of asynchronous interactions and heterogeneous configurations, which fails to achieve efficient parallel generation and constrains scalability in large-scale real-time applications. Multi-Agent Reinforced Training and Inference Framework (MARTI) [68] proposes the first unified multi-agent framework to support parallel training and inference, demonstrating that learned interaction patterns can guide LLMs toward more robust reasoning pathways. Building on this foundation, CoMAS [59] employs interaction-based intrinsic rewards to train multi-agent, significantly reducing the reliance on external supervision. Nevertheless, effectively unifying multi-agent cooperation and reflective search within RL paradigms remains challenging [75, 23, 76]. More crucially, the field still lacks a systematic evaluation of the evolutionary trajectory from single agents to homogeneous multi-role paradigms and subsequently to heterogeneous multi-agent paradigms, which limits our empirical understanding of how collective intelligence scales.

Therefore, building upon MARTI, we propose a Multi-Agent Reinforced Training and Inference Framework with Self-Search Scaling method (MARTI-MARS², denoted as MARS²), which conducts large-scale RL training to systematically explore the scaling laws of multi-agent systems. We posit that multi-agent collaboration serves as a critical axis for performance scaling, where optimized interactions can yield consistent gains beyond the limitations of single-model parameters or data. Specifically, MARS² deeply integrates hierarchical multi-agent tree search based on multi-turn refinement with policy learning. As shown in Figure 2, MARS² is designed to foster multi-agent co-evolution, which supports both parameter-sharing homogeneous multi-role agents and parameter-independent heterogeneous agents. During the training phase, we model the multi-agent collaborative search process as a learnable dynamic environment, enabling agents to acquire high-quality trajectories for improving fundamental reasoning ability through RL. Bridging to the inference phase, we further introduce an enhanced multi-agent TTS method MARS²-T+. Based on structured error feedback, dynamic depth-guided exploration, and reward model guidance in multi-agent system, MARS²-T+ fully exploit the scaling potential of multi-agent collaboration at test time. As illustrated in Figure 1, MARS² reveals multi-agent scaling laws: **the transition from single-agent to homogeneous multi-role (Homo-MARS²), and ultimately to heterogeneous multi-agent paradigms (Heter-MARS²), sequentially yields higher RL performance ceilings, stronger TTS capabilities, and greater diversity in the corresponding policies.** The paper collectively suggest a crucial insight: **integrating heterogeneous multi-agent scaling with RL paradigms represents a vital evolutionary trajectory beyond homogeneous multi-role paradigms, aiming to synthesize diverse cognitive capabilities.**

The main contributions are as follows:

- We conduct the first systematic large-scale training and scaling analysis of heterogeneous multi-agent systems in complex reasoning tasks, revealing that multi-agent collaboration via RL represents the next frontier of the scaling law beyond TTS. Extensive experiments on 8B, 14B, and 32B models uncover a robust performance hierarchy driven by interaction diversity: under equal computational budgets, the transition from a single agent to a parameter-sharing homogeneous multi-role paradigm yields initial performance gains (Section 3.2). Advancing to a parameter-independent heterogeneous

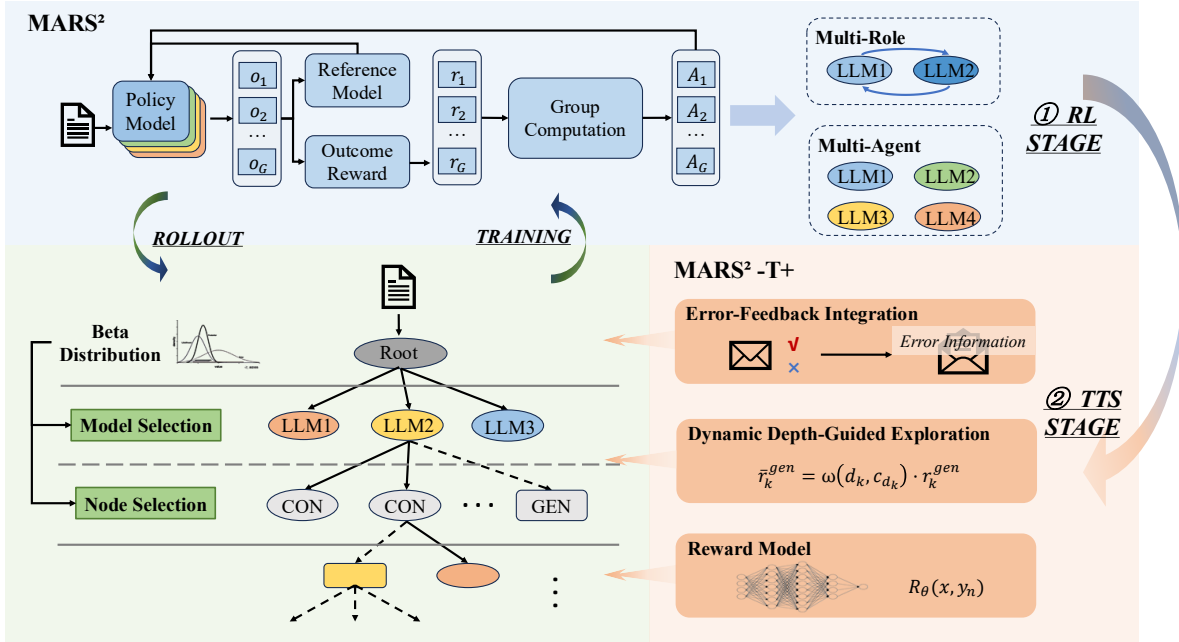


Figure 2: The framework of MARTI-MARS². In RL stage, the multi-role and multi-agent tree search is modeled as a learnable dynamic environment, enabling agents to improve reasoning capabilities via tree-based GRPO algorithm. In TTS stage, an enhanced method MARS²-T+ is introduced, incorporating error message feedback, dynamic depth-guided exploration, and pre-trained reward model to achieve efficient inference.

multi-agent paradigm further elevates the performance upper bound (Section 3.3). The findings confirm that trained multi-agent collaboration provides a scalable pathway capable of surpassing the performance limits of individual agents.

- We propose MARTI-MARS², a unified framework that bridges collaborative multi-agent training with inference scaling. By allowing multiple agents to actively explore and refine within a dynamic environment, MARS² facilitates a crucial evolution from parameter-sharing homogeneous multi-role training to heterogeneous multi-agent training, thereby breaking through the capability limits of single-agent optimization (Section 2.2). Complementing these training paradigms, we introduce MARTI-MARS²-T+ to fully exploit the scaling potential of multi-agent collaboration with reduced computational overhead through efficient guidance and refinement (Section 2.3). The framework demonstrates that leveraging two collaborating 32B models, MARS² achieves a performance of 77.7%, surpassing strong baselines such as O4-Mini (high) and GPT-5.1.
- We provide a granular analysis of diversity scaling in multi-agent collaboration, demonstrating that the progression from single-agent to homogeneous multi-role and finally to heterogeneous multi-agent paradigms progressively elevates strategic diversity alongside performance. To comprehensively assess this, we design multi-layered evaluations that measure diversity across semantics, algorithms, and cognitive reasoning (Section 4). This analysis confirms that the multi-agent performance scaling observed in our experiments is driven by the system’s enhanced capacity to discover diverse, high-quality reasoning paths, establishing diversity as a distinct and critical dimension of scaling beyond mere computational power.

2 Method

2.1 Overview

MARS² establishes a unified training and inference framework centered on multi-agent self-search. The framework consists of a structured multi-agent search and policy-update process during training, and a

reward-model-guided inference process, both operating on a shared tree-search structure (Figure 2). During training, MARS² employs cooperative multi-agent tree search to generate structured reasoning trajectories. Different layers of the search tree correspond to different sub-tasks of the reasoning process, and multiple agents jointly expand nodes, propose candidates, and produce multi-path reasoning sequences. These trajectories and their associated expansion paths are then used to update the policy model, forming a tree-search-driven pipeline for trajectory generation and policy learning. During inference, MARS² applies a reward model (RM)—trained on trajectories collected during training—to evaluate the final candidate solutions. The RM provides a learned evaluation signal, enabling the system to select outputs that are more consistent with task objectives while preserving the underlying search procedure.

2.2 The training paradigm of MARS²

The overall workflow of MARS² training phase can be summarized as follows: (i) collecting interaction data and reward signals, (ii) computing advantages and performing data preprocessing, (iii) distributing data to agents and dynamically updating agent parameters. Specifically, during the rollout phase, multiple agents are incorporated into the tree search process to obtain training data for each agent. For every sample, the expansion is applied to generate a more diverse trajectory tree. The groups originally formed through repeated sampling in GRPO [49] are replaced with groups represented by complete trajectory trees. Based on these trees, we collect rewards and compute advantages. The processed data are then assigned to the corresponding agent buffer according to the agent identifier. Once the size of an agent’s buffer reaches a predefined threshold, a parameter update for that agent is dynamically triggered.

2.2.1 Multi-Agent Instantiation

Within the unified tree-search framework, MARS² supports two multi-agent configurations: Homogeneous Multi-Agent (**Homo-MARS²**) and Heterogeneous Multi-Agent (**Heter-MARS²**). In the Homo-MARS² setup, all agents share the same policy parameters, and behavioral differences arise solely from the distinct system prompts and local contexts of the search tree. In contrast, the Heter-MARS² setup assigns each agent an independent set of parameters, naturally introducing higher policy diversity and complementary behaviors during collaborative search. Both configurations integrate seamlessly into the same tree-search procedure, enabling MARS² to maintain a consistent search structure while flexibly adjusting the agents’ heterogeneity based on task demands.

2.2.2 Data Collection and Advantage Calculation

During the rollout phase, the algorithm dynamically selects different agents $\mathcal{A}_j, j \in \{1, \dots, m\}$, where m denotes the total number of agents, to perform trajectory tree expansion. As each node is expanded, the code validation environment provides immediate feedback in the form of a scalar reward r : a reward of 1 is assigned if all test cases pass, and 0 if any test case fails. During training, all test cases are used to construct the training data. In contrast, during evaluation, we distinguish between public and private test cases: public test cases provide reward signals to guide the trajectory expansion, whereas private test cases are used solely for reporting the final evaluation results.

Reward Collection. For a given problem q , after the rollout stage is completed, we obtain a set of node information $\{\Pi_{\mathcal{N}_1, \mathcal{A}_{j_1}}, \Pi_{\mathcal{N}_2, \mathcal{A}_{j_2}}, \dots, \Pi_{\mathcal{N}_{G_T}, \mathcal{A}_{j_{G_T}}}\}$, where G_T represents the number of tree nodes, and the subscript $j_k \in \{1, \dots, m\}$ denotes the agent ID selected at node \mathcal{N}_k . After generating a response using agent \mathcal{A}_{j_k} at Node \mathcal{N}_k , node information $\Pi_{\mathcal{N}_k, \mathcal{A}_{j_k}}$ is created, containing the input prompt p_{k, j_k} , output sequence o_{k, j_k} , agent ID j_k , and the corresponding scalar reward r_{k, j_k} , which reflects the correctness of the code generated by the agent \mathcal{A}_{j_k} at node \mathcal{N}_k .

Advantage Calculation. To measure the relative advantage, we treat all nodes in the entire tree as a single group. Unlike GRPO, which evaluates the state-action pairs of individual agent, our setting focuses on the relative performance of the entire multi-agent system. Although the group contains the inference results of multiple agents, we can still use the formula (14) to compute the advantage at the group-level, quantifying the relative advantage of each agent within the group, which helps agents identify their strengths and weaknesses compared to other agents, providing better guidance for their learning and development. Therefore, the advantage of all tokens gained by the selected agent \mathcal{A}_{j_k} at node \mathcal{N}_k is:

$$\hat{A}_{k,t}^{j_k} = \hat{A}_{k,t} = \frac{r_{k,j_k} - \text{mean}(r_{1,j_1}, r_{2,j_2}, \dots, r_{G_T,j_{G_T}})}{\text{std}(r_{1,j_1}, r_{2,j_2}, \dots, r_{G_T,j_{G_T}})} \quad (1)$$

2.2.3 Data dispatching and Dynamic Training

Distributing Data. After calculating the inter-group advantages $\{\hat{A}_{1,t}^{j_1}, \hat{A}_{2,t}^{j_2}, \dots, \hat{A}_{G_T,t}^{j_{G_T}}\}$ for each node, based on the formula (1), the results are incorporated into the node information $\{\Pi_{\mathcal{N}_1, \mathcal{A}_{j_1}}, \Pi_{\mathcal{N}_2, \mathcal{A}_{j_2}}, \dots, \Pi_{\mathcal{N}_{G_T}, \mathcal{A}_{j_{G_T}}}\}$. Since the nodes in the tree correspond to different agents, we add the node information $\Pi_{\mathcal{N}_k, \mathcal{A}_{j_k}}$ to the experience buffer \mathcal{B}_{j_k} of the corresponding agent for subsequent training.

Asynchronously triggered Dynamic Training. During multi-agent tree search, each node is expanded by dynamically selecting an agent according to an updatable Beta prior. Although the total amount of data collected per rollout is fixed, the data received by each agent is highly imbalanced across rollouts, causing different agents to accumulate data at different rates. Using synchronous updates under such conditions would lead to waiting and blocking, reducing system throughput and computational efficiency. To address this issue, we introduce a dynamically and asynchronously triggered training mechanism: each agent maintains its own data buffer, and a parameter update is triggered only when that agent's buffer reaches a predefined threshold, without requiring synchronization with other agents.

2.2.4 The optimization objective of MARS²

MARS². Each sample stored in an agent's buffer already contains all variables required for training, including the complete input–output pair, the action mask, the associated log-probability information, and the normalized intra-group advantage computed using Eq. 1. Once the buffer size reaches the predefined threshold, these data can be directly used for training under the GRPO optimization objective in Eq. 15. Building on this foundation, we further introduce an optimization objective tailored to MARS² setting.

$$\begin{aligned} \mathcal{J}_{\text{MARS}^2}(\Theta) = \mathbb{E}_{q \sim \mathcal{D}, \{o_i\}_{i=1}^{\mathcal{C}_{\text{Tree}}} \sim \pi_{\Theta_{\text{old}}}(\cdot | q)} & \left[\sum_{j=1}^m \frac{1}{\sum_{\hat{A}_i \in \mathcal{B}_j} |o_i|} \sum_{\hat{A}_i \in \mathcal{B}_j} \sum_{t=1}^{|o_i|} \right. \\ & \left(\min \left(w(i, t, \theta_j) \hat{A}_{i,t}, \text{clip} \left(w(i, t, \theta_j), 1 - \epsilon_{\text{low}}, 1 + \epsilon_{\text{high}} \right) \hat{A}_{i,t} \right) \right. \\ & \left. \left. - \beta \text{D}_{\text{KL}}(\pi_{\theta_j} \| \pi_{\text{ref}}) \right) \right], \end{aligned} \quad (2)$$

where we adopt the group-based advantage estimation for $\hat{A}_{i,t}$ by the equation 1, and denote $\Theta = \{\theta_1, \theta_2, \dots, \theta_m\}$ as the parameters set of all agents. The importance ratio is defined as

$$w(i, t, \theta_j) = \frac{\pi_{\theta_j}(o_{i,t} | q, o_{i,<t})}{\pi_{\theta_j, \text{old}}(o_{i,t} | q, o_{i,<t})}.$$

MARS²⁺. In practice, we observed that the aforementioned optimization objective performs suboptimally in reinforcement learning for long-chain reasoning models, often resulting in performance stagnation or deterioration. This issue is particularly pronounced in complex tasks such as code generation. To stabilize multi-agent training, we analyzed the failure cases encountered in our experiments and leveraged prior work on reinforcement learning stabilization [73, 64, 61]. Guided by these findings, we introduce the MARS²⁺

optimization objective:

$$\begin{aligned} \mathcal{J}_{\text{MARS}^2+}(\Theta) = \mathbb{E}_{q \sim \mathcal{D}, \{o_i\}_{i=1}^m \sim \pi_{\Theta_{\text{old}}}(\cdot|q)} \left[\sum_{j=1}^m \frac{1}{\sum_{\hat{A}_i \in \mathcal{B}_j} |o_i|} \sum_{\hat{A}_i \in \mathcal{B}_j} \sum_{t=1}^{|o_i|} \right. \\ \left. \text{vllm_kl}(j) \left(\min \left(s(i, j, \theta_j) \hat{A}_{i,t}, \text{clip} \left(s(i, j, \theta_j), 1 - \epsilon_{\text{low}}, 1 + \epsilon_{\text{high}} \right) \hat{A}_{i,t} \right) \right. \right. \\ \left. \left. - \beta \mathbb{D}_{\text{KL}}(\pi_{\theta_j} \parallel \pi_{\text{ref}}) \right) \right], \end{aligned} \quad (3)$$

Specifically, MARS² is extended with three components—GSPO, Overlong Penalty, and TIS [73, 64, 61] that mitigate factors causing instability in training from different perspectives:

- **GSPO.** Although GSPO [73] was originally proposed to stabilize Mixture-of-Experts (MoE) model training, our experiments indicate that it is also crucial for stabilizing long-chain reasoning in dense models. By applying a geometric mean over the importance weights across the entire reasoning chain, GSPO smooths the influence of unstable tokens:

$$s(i, j, \theta_j) = \left(\frac{\pi_{\theta_j}(o_i|x)}{\pi_{\theta_{j,\text{old}}}(o_i|x)} \right)^{\frac{1}{|o_i|}} = \exp \left(\frac{1}{|o_i|} \sum_{t=1}^{|o_i|} \log \frac{\pi_{\theta_j}(o_{i,t}|x, o_{i,<t})}{\pi_{\theta_{j,\text{old}}}(o_{i,t}|x, o_{i,<t})} \right).$$

- **Overlong Penalty.** Through case study, we observed that most poor responses were truncated outputs. To address this, we adopted the reward shaping strategy used in DAPO [64] to penalize overlong and incorrect responses, thereby discouraging this behavior:

$$R_{\text{length}}(y) = \begin{cases} 0, & |y| \leq L_{\text{max}} - L_{\text{cache}} \\ \frac{(L_{\text{max}} - L_{\text{cache}}) - |y|}{L_{\text{cache}}}, & L_{\text{max}} - L_{\text{cache}} < |y| \leq L_{\text{max}} \\ -1, & L_{\text{max}} < |y| \end{cases}$$

- **TIS.** To alleviate the instability caused by the mismatch between inference and training parameters, we applied the same mitigation strategy as described in TIS [61] to ensure consistent reasoning behavior during training:

$$\text{vllm_kl}(j) = \log \left(\frac{\pi_{\theta_j}^{\text{vllm}}(o_i|q)}{\pi_{\theta_j}^{\text{fsdp}}(o_i|q)} \right)$$

2.3 Test Time Scaling of MARS²

During training, the rollout procedure uses the full set of test cases to provide precise feedback, whereas inference must rely solely on public test cases, resulting in a clear discrepancy between training-time and test-time supervision. In addition, we observe that vanilla TTS such as AB-MCTS method [19] lacks fine-grained intermediate feedback during the search process, often leading to insufficient refinement and inaccurate evaluation of certain branches, which ultimately hampers inference performance. To mitigate these limitations, we introduce MARS²-T+, which incorporates two key components: (i) a multi-agent, refinement-enhanced search mechanism that improves intermediate reasoning quality during inference, and (ii) a Reward Model (RM) trained on data collected in the training phase to provide more reliable scoring of final candidates, thereby partially bridging the feedback gap between training and inference.

2.3.1 Multi-Agent Refinement-based tree search

While adaptive tree-search strategies have improved the balance between exploration and exploitation in test-time scaling, they still fall short of fully leveraging the potential of collaborative reasoning in multi-agent settings. Our experiments reveal two key limitations of these methods when applied to complex code generation tasks: (1) **Insufficient error utilization**; (2) **Limited depth for refinement**. These limitations are

particularly critical in multi-agent systems, as effective coordination and cross-agent feedback are essential for problem solving. Further empirical validation is provided in Appendix B.3.

To address these limitations, we propose multi-agent refinement-based tree search (MARS²-T+). Our approach adopts the model selection and node expansion mechanisms from Multi-Agent AB-MCTS, while integrating two lightweight yet highly effective mechanisms to encourage multi-agent systems to perform more precise and deeper refinement. Specifically, our method enhances the quality of inter-agent interactions through the error-feedback integration mechanism, which provides fine-grained diagnostic signals, and increases the frequency of such interactions through dynamic depth-guided exploration, which drives the search toward greater depth.

Error-Feedback Integration. When a node N fails validation, our method augments its subsequent refinement steps with structured diagnostic feedback. This feedback includes a unified set of general signals—an execution summary, the error message, and the corresponding error code—followed by error-type-specific context. For Wrong Answer cases, we provide the failed input–output pairs along with the expected outputs on the public test; for execution errors (e.g., `IndexError`, `TimeoutError`), we provide the error type and detailed error trace. This structured formulation enables the selected agent to reason about the underlying cause of failure rather than merely perturbing previous outputs. Importantly, the enhanced feedback is injected only during the refinement phase to preserve the diversity of initial exploration. Additional prompting details are provided in Appendix C.1.

Dynamic Depth-Guided Exploration. Our experiments reveal that many unresolved cases stagnate in shallow regions of the search tree, where the system fails to exploit the collaborative potential of the multi-agent setting. To encourage deeper interaction among agents, we introduce a depth-aware bias into the Thompson sampling scores for the GEN action. Specifically, let d denote the depth of the node being expanded, and let c_d denote the number of nodes already generated at depth d . We modulate the original Thompson sampling score using a weighting function $w(d, c_d)$ that depends on both the depth and the node count at that depth:

$$\tilde{r}_k^{\text{gen}} = w(d_k, c_{d_k}) \cdot r_k^{\text{gen}}, \quad (4)$$

where r_k^{gen} is the Thompson sample for selecting the GEN action at node k . We compute the weighting function using the following formulation:

$$w(d_k, c_{d_k}) = \gamma(d_k)^{c_{d_k}} \quad (5)$$

where $\gamma \in (0, 1)$ is a depth-dependent decay factor. In our experiments, $\gamma(d_k)$ is assigned a value close to 1 at shallow depths (e.g., $\gamma(1) = 0.98$) and is designed to gradually decay as d_k increases, thereby encouraging broad exploration during the early stages of search and progressively guiding the algorithm toward deeper and more focused exploration as the tree grows.

2.3.2 Reward Model of MARS²-T+

Although the environment provides a definitive binary reward $r \in \{0, 1\}$, this reward signal is inherently **sparse**. Crucially, this sparsity is severely compounded by the reward’s reliance on a limited set of **public test cases**. This limitation often leads to a phenomenon we term “**reward hacking**”: solutions ($r = 1$) which overfit the public tests and fail in comprehensive, hidden private tests. Furthermore, when multiple solutions pass the public tests, the sparse $r = 1$ signal is insufficient to distinguish their actual robustness, thus severely impeding the final pass@1 performance.

To furnish a more fine-grained estimation of node quality that truly correlates with private test success, we construct a dedicated Reward Model (RM), $R_\theta(x, y)$, trained to predict the probability of a given solution y passing the problem’s private test cases. Our implementation features a complete RM pipeline, detailing the training process (including data construction, objective optimization and benchmark) before demonstrating the model’s integration into the multi-agent tree search.

Training Data Construction. The foundation of a reliable RM is a large-scale dataset of code solutions with known outcomes. We curate this dataset by leveraging our policy models (agents) as the data generation engine, using the DeepCoder dataset as the problem pool. Further details on data collection and formatting are available in Appendix C.1.

Training Objectives. We initialize our RM R_θ from the Skywork-Reward-V2-Qwen3-8B[33] checkpoint. The model takes (x, y) as input and outputs a scalar score $s = R_\theta(x, y)$. We apply a sigmoid function $\sigma(\cdot)$ to the output score and optimize against the binary ground-truth label r using the Mean Squared Error (MSE) Loss. Other objectives are discussed in Appendix C.2.

$$L_{MSE} = (\sigma(R_\theta(x, y)) - r)^2 \quad (6)$$

Benchmark Construction for RM Evaluation. To rigorously evaluate our trained RM, we constructed several evaluation benchmarks from held-out datasets (LiveCodeBench_v6). The detailed generation process, benchmark statistics, and evaluation metrics (e.g., Pairwise Accuracy, MSE) are deferred to Appendix C.3.

Application of RM in MARS²-T+. In our MARS²-T+ algorithm, the RM serves as a decisive selector for the final solution rather than a heuristic guiding the search process. Specifically, we focus on the set of candidate nodes \mathcal{N}_{pass} that successfully pass the public tests (i.e., $r_n = 1$). Within this functionally correct subset, we invoke the RM to evaluate the quality of each solution. The final solution y^* is determined by selecting the node with the highest RM score:

$$y^* = \arg \max_{n \in \mathcal{N}_{pass}} R_\theta(x, y_n) \quad (7)$$

where $R_\theta(x, y_n)$ denotes the continuous prediction score from the RM for the solution y_n at node n . This mechanism ensures that the algorithm prioritizes solutions that are not only verified by public tests but also aligned with the RM’s quality estimation, thereby maximizing the probability of passing hidden private tests.

3 Experiments

3.1 Experimental Setup

Base LLMs Policies. To comprehensively evaluate the performance of MARS² in code generation, we construct open-source model pool with parameter scales of 8B, 14B and 32B, encompassing seven recently released representative LLMs. For code-oriented LLMs, we select **AReAL-boba-2 8B/14B** [14] and **DeepCoder-14B-Preview** [40] to verify that MARS² remains an effective enhancement method for improving code generation capabilities, even in models that have already been extensively optimized for code-related tasks. Additionally, we incorporate the general LLMs **Qwen3 8B/14B/32B** [60] and **Nemotron 32B** [1] to further demonstrate the generalizability and universality of our method.

Training Dataset. We select the open-source coding dataset released by DeepCoder [40] as the foundation for training data. To optimize training efficiency, we systematically filter two types of extreme samples: those for which the model’s solutions achieve a perfect score and those for which the solutions receive a zero score. Following this filtering strategy, a training dataset comprising 7,992 coding prompts is constructed. RL training for our proposed method and all baselines are based on this dataset.

Baseline. To verify the effectiveness of MARS² and reveal the multi-agent scaling law, we adopt vanilla GRPO as the single-agent baseline. To ensure that no additional RL-specific tricks bias the results, we incorporate the same RL techniques described in Section 2.2 into the vanilla GRPO setup.

Evaluation Benchmark and Metrics. For evaluation, we adopt **LiveCodeBench(v6, 01/25-05/25)** [20] as our benchmark (LCB), which is released after the development of the base LLMs to guarantee the absence of data leakage. Besides, we choose three principal evaluation metrics to comprehensively evaluate the performance of MARS² from different dimensions and demonstrate the multi-agent scaling law.

1. **Pass@1.** We employ Pass@1 as the primary metric to assess the LLMs fundamental reasoning and code generation capabilities before and after RL, which measures the probability that the LLM generates a correct solution in a single sampling attempt. This metric directly reflects the improvement in individual capabilities of LLMs based on MARS².
2. **Pass@1(MCTS).** During the TTS phase, we conduct N complete rollouts in the structured environment established by MARS² using tree search. Among these N candidate solutions, the optimal one (such as the solution with the highest score from the reward model or the first to pass the test) is selected for final evaluation as the result, which are denoted as Pass@1(MCTS). The metric reflects the effectiveness of our method in enhancing system performance through structured search during inference.

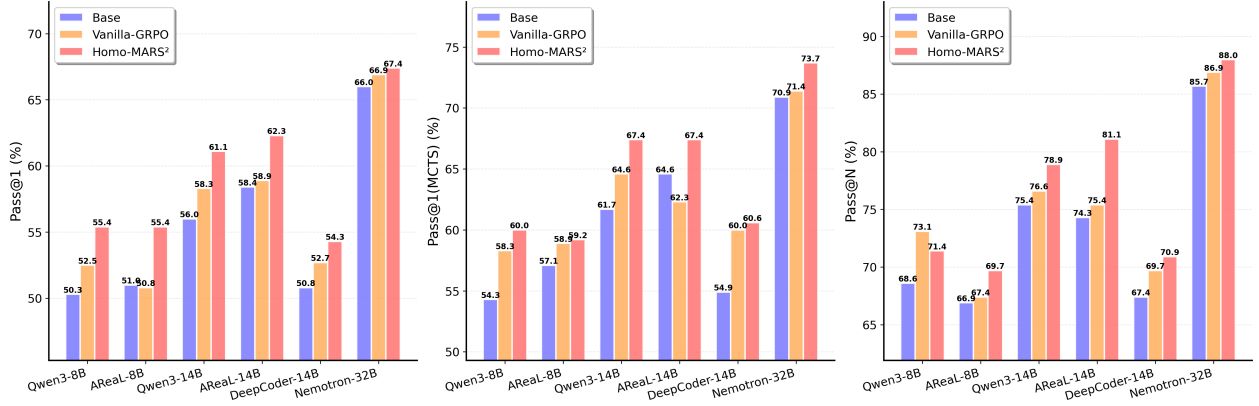


Figure 3: Experimental results of Homo-MARS² and baseline methods on LCB benchmarks. The inference budgets are $N = 60$.

3. **Pass@N**. The PASS@N metric evaluates the probability that at least one of N generated solutions passes all unit tests. This metric not only indicates the LLMs average performance but also reflects its capacity to generate both effective and diverse solutions.

Training Details. We extend MARTI [68] framework to conduct both single-agent and multi-agent RL. For single-agent training, we use one node equipped with eight H200 GPUs. For multi-agent training, we use a cluster consisting of as many nodes as the number of agents, with each node containing eight H200 GPUs, and each agent occupying one full node. The complete set of training hyperparameters is summarized in Appendix A.1.

3.2 Results of Homo-MARS²

Takeaway

- (1) **Significant performance boost & Faster convergence.** Homo-MARS² effectively broadens the search space by aggregating the experiences of homogeneous multi-role agents, thereby enhancing the performance ceiling and convergence speed of RL. Even for specialized code LLMs where traditional optimization methods struggle to improve or may even degrade performance, Homo-MARS² is still able to achieve significant performance gains.
- (2) **Late-stage bottleneck from homogeneity.** Despite the remarkable initial results, parameter sharing among homogeneous agents leads their policies to rapidly converge. This loss of diversity restricts continued exploration and further performance improvements in the later stages of training, prematurely resulting in performance stagnation.

To investigate the effectiveness of the MARS² training paradigm, we first conduct comprehensive experiments based on a homogeneous multi-role setting (Homo-MARS²) for base LLMs policies with 8B, 14B, and 32B parameters. In this setting, all homogeneous agent roles share the same set of parameters and collaborate in exploration and policy learning. To ensure fairness in comparison, all reported performance metrics were measured at the same number of training steps. Detailed experimental results are presented in Figure 3.

Higher performance and faster convergence speed. The experimental results demonstrate that Homo-MARS² surpasses the baseline method across five distinct base LLMs policies. Specifically, regarding individual model capabilities, Homo-MARS² achieved the highest Pass@1 scores on all models, yielding a significant performance gain of up to 4.6% over Vanilla GRPO. In terms of system-level search performance, the Pass@1(MCTS) metric improves by as much as 5.1%, which strongly indicates that policies trained by Homo-MARS² more effectively guide MCTS toward optimal solutions. As illustrated in Figure 4a, the training curve for Homo-MARS² exhibits faster convergence and superior performance in the early stages, attributable to its multi-role exploration mechanism. The method enables homogeneous multi-role agents to explore the solution space from diverse perspectives and aggregates their successful experiences through a shared parameter pool. Homo-MARS² substantially broadens the exploration scope, thereby facilitating the

efficient discovery and utilization of high-quality training trajectories.

Stronger deep optimization capabilities. It is noteworthy that the performance of LLMs that specifically designed for code tasks (such as AReal and DeepCoder), shows relatively limited potential for improvement through traditional optimization methods like Vanilla-GRPO. As indicated in Figure 3, Vanilla-GRPO even led to a slight performance degradation in the Pass@1 metric for the AReal-8B, decreasing from 51.0% to 50.8%. However, by overcoming the limitations of a single optimization trajectory and thus effectively avoiding local optima, Homo-MARS² still achieves significant performance gains on these models.

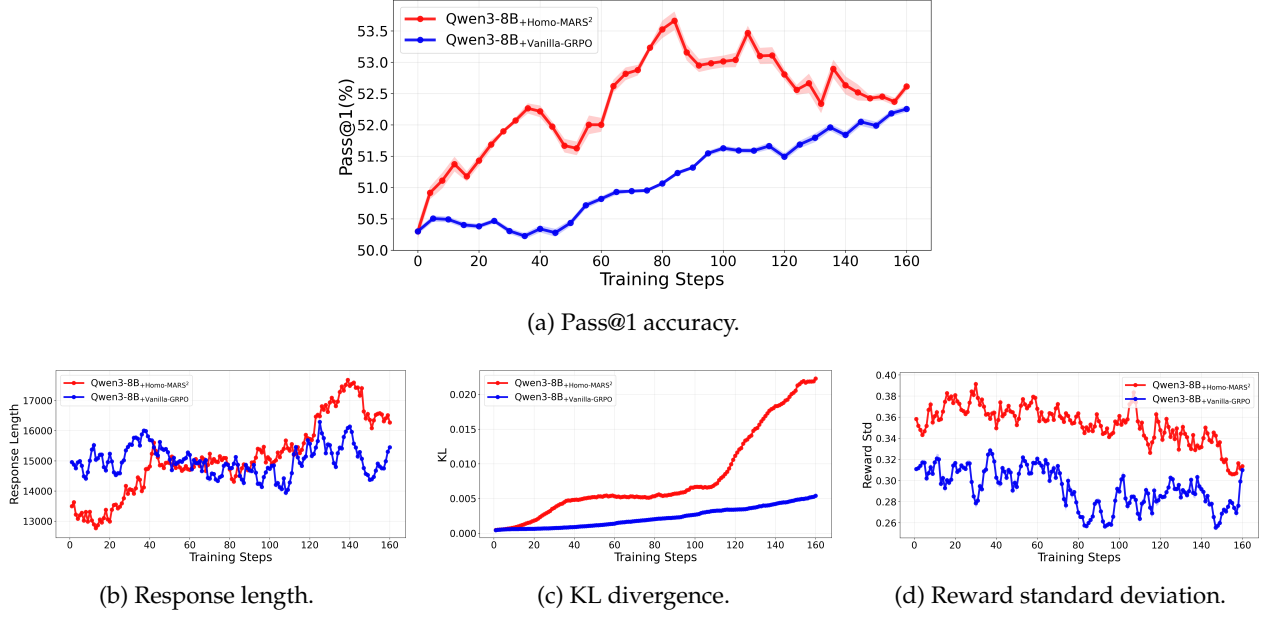


Figure 4: Performance of Homo-MARS² and GRPO on Qwen3-8B across training steps.

The inherent limitations of Homo-MARS². As the number of training steps increases, we observe a key phenomenon: after Homo-MARS² reaches an early performance peak, its improvement stagnates and even exhibits a slight decline in later stages, as shown in Figure 4a. Due to parameter sharing among homogeneous multi-role agents, they tend to learn similar strategies and behavioral patterns during training, leading to policy homogeneity. While such convergence in strategies facilitates rapid aggregation of effective experiences and performance gains in the early training phase, it subsequently constrains the diversity of exploration. As illustrated in Figure 4d, the reward standard deviation of Homo-MARS² drops significantly in the later stages, indicating that the agents' explored strategy returns become increasingly homogeneous, thereby reducing diversity. This causes the policy network to prematurely converge to a local optimum, resulting in a performance bottleneck for Pass@1. Meanwhile, Homo-MARS² tends to become unstable in the later training stages. As shown in Figures 4b and 4c, there is a marked and unnecessary increase in both response length and KL divergence. This suggests that, when exploration capacity is limited, the LLMs may attempt to achieve performance breakthroughs by forcibly generating longer responses or deviating further from the initial policy, which instead leads to behavioral degradation and unstable performance.

Therefore, although Homo-MARS² demonstrates the potential of the multi-agent framework in the initial phase of training, its homogeneous characteristic also presents new challenges for the model's continuous optimization.

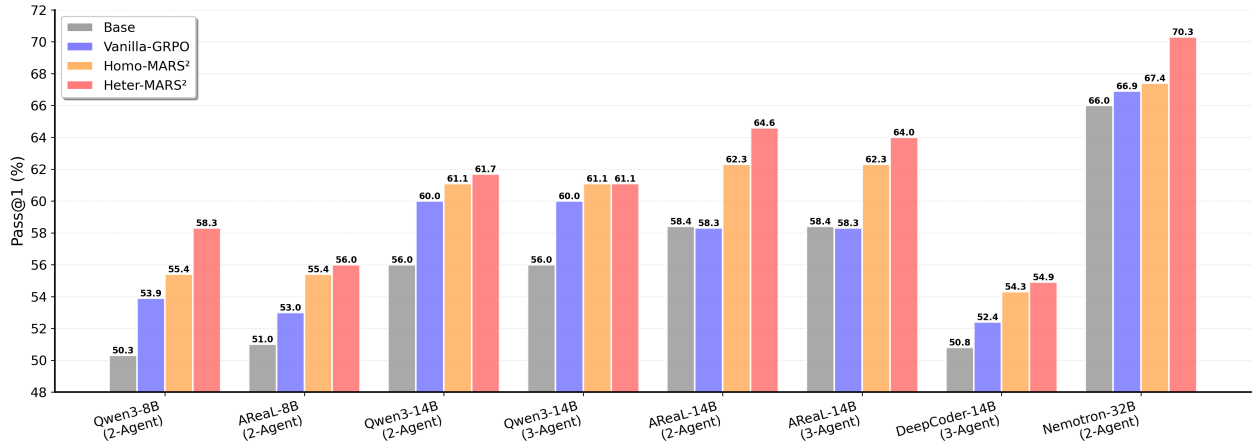


Figure 5: Pass@1 results of Heter-MARS² and baseline methods on LCB benchmarks.

3.3 Results of Heter-MARS²

Takeaway

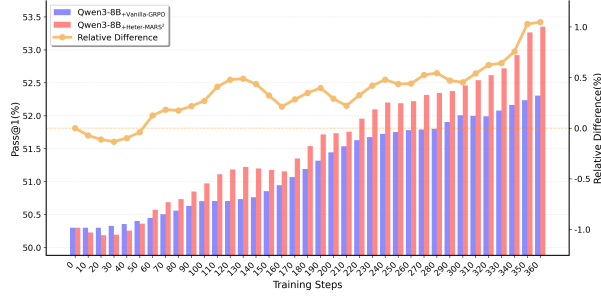
- (1) **Breaking Through Individual Performance Ceilings.** Heter-MARS² compels each agent to explore a broader solution space to adapt to dynamically changing peer policies, which leads to superior and more stable individual performance.
- (2) **Enhancing Group Collaboration Efficiency.** At the system level, through complementarity and error correction among diverse strategies, heterogeneous multi-agent systems demonstrate high-quality collaborative problem-solving capability. Their collective performance significantly surpasses that of any single agent or homogeneous team.
- (3) **Revealing Multi-Agent Scaling Law.** Heter-MARS² demonstrates that scaling up agent diversity and interaction complexity serves as a powerful, orthogonal pathway to increasing model parameters. This finding establishes multi-agent collaboration as an effective paradigm for extending the reasoning frontiers of LLMs.

To address the performance bottleneck caused by strategy convergence in Homo-MARS² during the later stages of training, we propose a superior training framework Heter-MARS². In this framework, each agent is assigned an independent parameter set, thereby ensuring a high degree of strategy diversity throughout the exploration and learning processes. This design elegantly models the heterogeneous multi-agent tree search process as a learnable dynamic environment, endowing the system with enhanced adaptability and exploration capabilities.

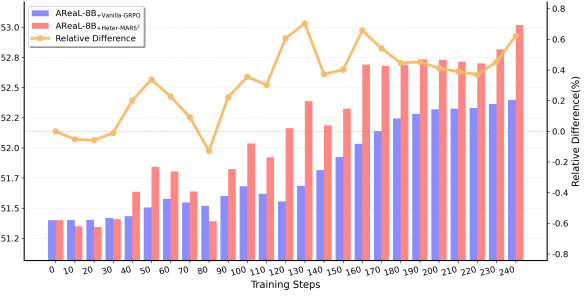
For a comprehensive and equitable evaluation of the effectiveness of Heter-MARS², we construct multi-agent ensembles using LLMs of 8B and 14B scales for experimentation. In the comparative analysis, we strictly ensure that the total amount of training data utilized by different methods is identical. Notably, given the performance degradation and instability exhibited by Homo-MARS² in the later stages of training, we select its best checkpoint during the entire training stages as final performance metric, thus enabling the most favorable comparison. Experimental results clearly demonstrate that the introduction of Heter-MARS² brings significant advantages: it not only effectively improves the system's performance ceiling and the efficiency of multi-agent collaboration, but also more profoundly unlocks the intrinsic potential of the base LLMs, achieving performance that surpasses Homo-MARS² and baseline methods.

Superior individual performance. To validate the effectiveness of Heter-MARS² in enhancing the performance of individual agents, we conduct comprehensive Pass@1 performance evaluations on five base LLMs, with the experimental results illustrated in Figure 5. The evaluation consistently demonstrates that agents trained with Heter-MARS² significantly and stably outperform the baselines and the Homo-MARS², which fully attests to the superiority and robustness of our proposed method. Taking Qwen3-8B as an example, there is a clear incremental improvement: the Pass@1 score of Heter-MARS² increased by 8.0% compared to the base model, by 4.4% over the Vanilla-GRPO baseline, and by 2.9% relative to the peak performance of

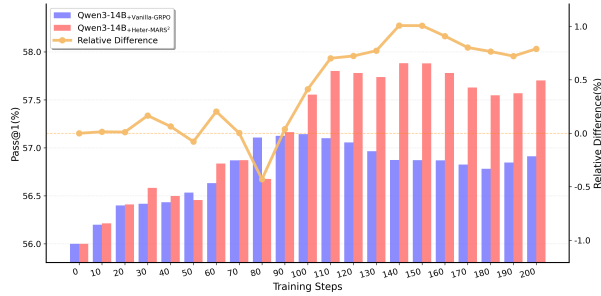
Homo-MARS².



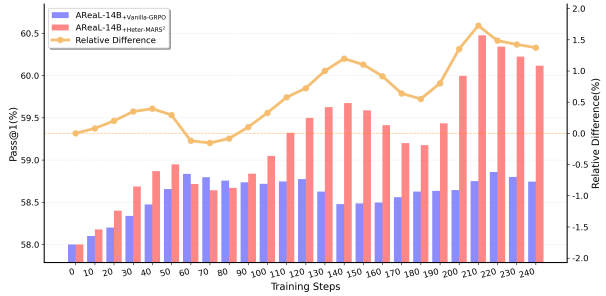
(a) Heter-MARS² and GRPO on Qwen3-8B.



(b) Heter-MARS² and GRPO on AReaL-boba-2-8B.



(c) Heter-MARS² and GRPO on Qwen3-14B.



(d) Heter-MARS² and GRPO on AReaL-boba-2-14B.

Figure 6: Scaling trend of generation budgets and agents across models and parameter sizes.

The progressive relationship in performance from Vanilla-GRPO to Homo-MARS² and then to Heter-MARS² reveals the influence of different training paradigms on the upper limit of individual capability. Vanilla-GRPO learns from single-agent exploration, which tends to lead to locally optimal strategies. Homo-MARS² introduces multi-role interaction and accelerates the learning process by leveraging parameter sharing, thereby outperforming Vanilla-GRPO. However, in such a homogeneous environment, strategies ultimately converge toward homogeneity, diminishing the exploratory value of the environment and thus limiting further improvement in individual performance. The core advantage of Heter-MARS² lies in its maintenance of strategy diversity, which constructs a continuously evolving heterogeneous interaction environment. In this setting, each agent must adapt to dynamic environments consisting of other agents employing distinct strategies. This heterogeneity-derived challenge forces individuals to explore a broader solution space to seek more robust strategies, effectively circumventing the performance saturation observed in homogeneous environments and elevating the upper bound of individual performance to a new level.

In order to conduct an in-depth analysis of the dynamic characteristics of Heter-MARS² during the training process, we compare its performance curve with the Vanilla-GRPO baseline. As shown in Figure 6, there are significant differences between the two methods in terms of learning efficiency and final performance. In the early stages of training, due to the need for heterogeneous agents to explore a vast policy space, the performance curve of Heter-MARS² exhibits certain fluctuations and a relatively slow rate of improvement. However, as training progresses, Heter-MARS² effectively avoids the problem of local optima through interaction and reflection among heterogeneous multi-agents, resulting in a continuously and steadily increasing performance curve that surpasses Vanilla-GRPO. This indicates that Heter-MARS² provides a more sustainable optimization pathway through maintaining policy diversity, thereby consistently elevating the performance ceiling of single-agent RL.

Enhanced multi-agent collaboration. In addition to enhancements in individual performance, Heter-MARS² significantly promotes superior system-level collaboration and feedback mechanisms, as demonstrated by its performance in the TTS stage shown in Figure 7. A heterogeneous agent team composed of Qwen3-8B and AReaL-8B, trained with Heter-MARS², achieved a Pass@1(MCTS) score of 62.3%, marking a notable increase of 5.2 percentage points compared to the base model (57.1%), and outperforming Vanilla-GRPO (58.3%) and Homo-MARS² (59.4%). Similarly, this upward trend can be observed in the 14B-level model combination, with Heter-MARS² achieving a maximum performance of 71.2%. Furthermore, the Pass@N metric exhibits

consistent and stable improvements, confirming the comprehensive enhancement of system collaborative problem-solving capabilities provided by our method.

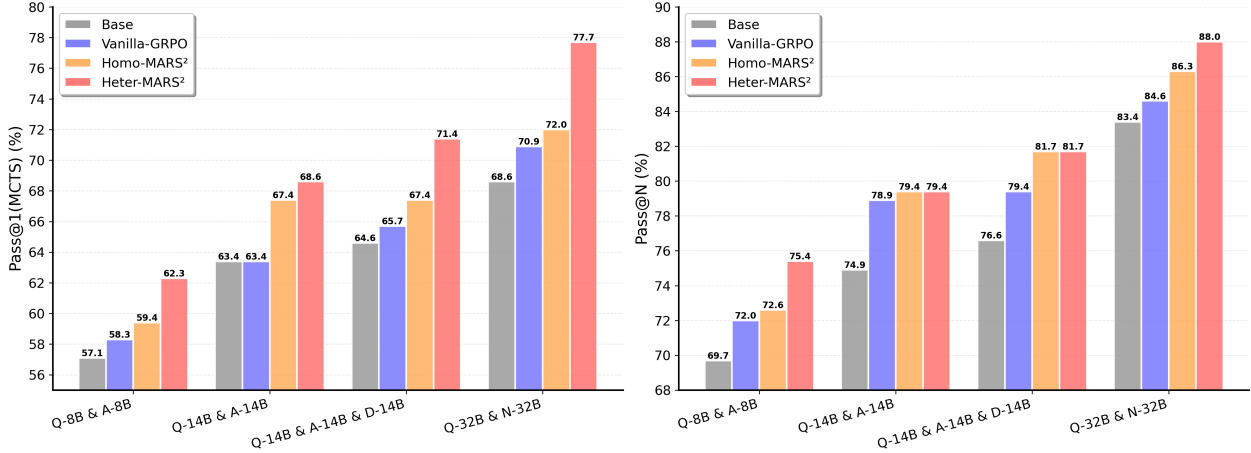


Figure 7: Pass@1(MCTS) and Pass@N results of Heter-MARS² and baseline methods on LCB benchmarks. The inference budgets are $N = 60$. For simplicity, Q denotes the Qwen3, A denotes the AReal, D denotes the DeepCoder, N denotes the Nemotron.

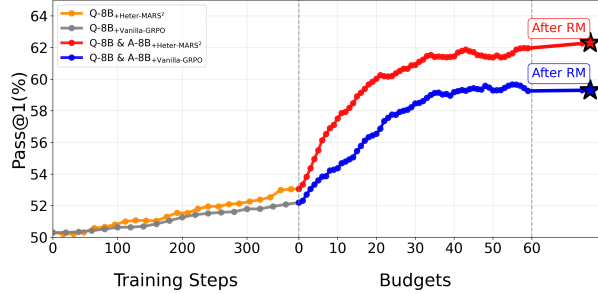
Specifically, Heter-MARS² enables multi-agent systems to surpass the simple aggregation of capabilities obtained through single-agent RL by leveraging interactions and feedback among heterogeneous agents. Different agents (such as Qwen3 and AReal) possess unique knowledge boundaries and reasoning inclinations, which are transformed into complementary advantages by Heter-MARS². Through high-quality “peer review”, multiple agents inspire and correct each other’s biases, collaboratively exploring more optimal problem-solving pathways.

Multi-dimensional collaborative scaling law. In order to further investigate the scalability enabled by Heter-MARS², we examined its performance at different stages, revealing a new dimension that transcends traditional scaling laws. As shown in Figure 8, we plot the performance curves during both the post-training phase and test-time phase, which compare Heter-MARS² and GRPO across various model combinations. The results clearly demonstrate the scaling phenomenon along two orthogonal dimensions:

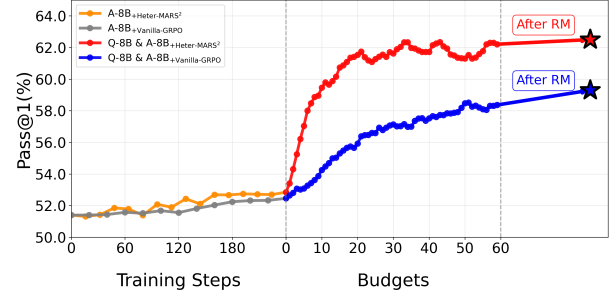
- **Scaling from post-training to test-time:** During the post-training phase, where no tree search is conducted and inference relies solely on the policy model, the system trained by Heter-MARS² already outperforms GRPO. This indicates that, through multi-agent interaction and feedback, the policy networks of the agents have been effectively optimized. When entering the test phase, the system undergoes collaborative tree search via MCTS, whose performance exhibits a second and more significant leap beyond post-training results. Heter-MARS² not only possess stronger individual capabilities, but also excel at surpassing higher performance limits during testing through collaborative exploration and feedback mechanisms. Notably, when our high-quality reward model is involved to guide the search process, the performance boost is further amplified, reaching the peak performance of the system.
- **Scaling from single-agent to multi-agent:** Whether in terms of policy capability at the post-training stage or collaborative ability at the test-time stage, the experimental results clearly demonstrate that the performance ceiling of multi-agents is significantly higher than that of any single-agent. The complementary knowledge and cross-validation mechanisms among heterogeneous agents break the capability bottleneck of individual models, enabling the entire system to solve more complex problems. This expansion from single-agent to multi-agent systems paves a parallel and complementary path for enhancing LLMs capabilities, alongside simply scaling up model size.

3.4 Results of MARS²-T+

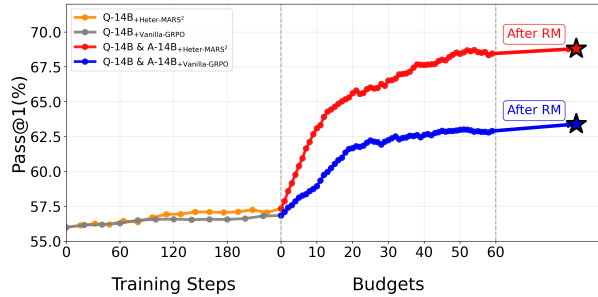
The Limitations of Vanilla-TTS. We begin by systematically evaluating the performance of Vanilla multi-agent tree search (Vanilla TTS) across a variety of models and model combinations. The results show that while Vanilla TTS provides modest system-level gains under small inference budgets, its improvements



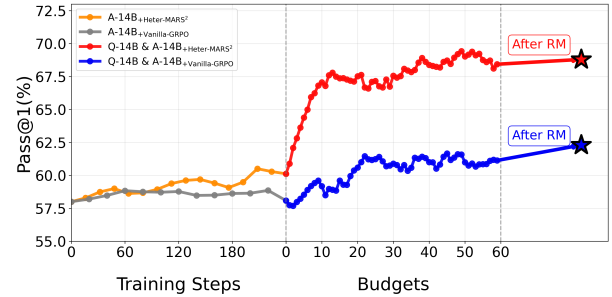
(a) Three-stage performance on Qwen3-8B.



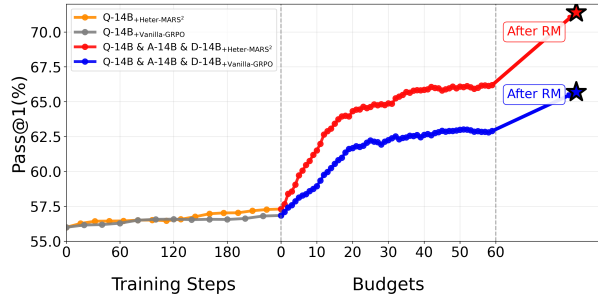
(b) Three-stage performance on AReaL-boba-2-8B.



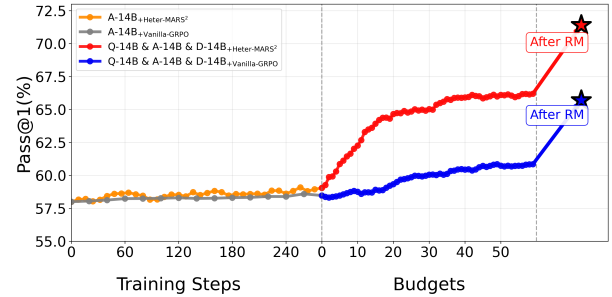
(c) Three-stage performance on Qwen3-14B.



(d) Three-stage performance on AReaL-boba-2-14B.



(e) Three-stage performance on Qwen3-14B.



(f) Three-stage performance on AReaL-boba-2-14B.

Figure 8: Three-stage scaling trend across different models and parameter sizes.

quickly saturate as the budget increases, revealing a clear upper bound (Figure 10 (Base)). A deeper analysis identifies three key limitations:

- **Insufficient exploitation of error signals.** As Appendix B.4 shows, Vanilla TTS supplies only binary "pass/fail" feedback from parent to child nodes, discarding richer diagnostic information such as input–output mismatches or runtime error logs. This coarse feedback is insufficient for guiding effective refinement in complex code-generation tasks.
- **Limited depth for refinement.** As shown in Figure 9, over 90% of nodes in the 14B model group remain within the first three levels of the search tree, with fewer than 7% reaching level four or deeper. This strong shallow bias becomes even more pronounced in multi-agent settings; even after the model is strengthened through MARS² training, the proportion of deeper nodes under Vanilla TTS remains very low, leaving substantial multi-agent collaboration potential underutilized.
- **Unstable candidate selection.** Vanilla TTS selects the last node that passes the public test cases as the final output. Because public test cases are sparse and cover only a narrow portion of the task space, this selection rule tends to favor solutions overfitted to visible examples. As illustrated in Figure 11, Pass@1(MCTS) exhibits substantial variance under increasing budgets and fails to deliver consistent improvements even when the compute budget is doubled.

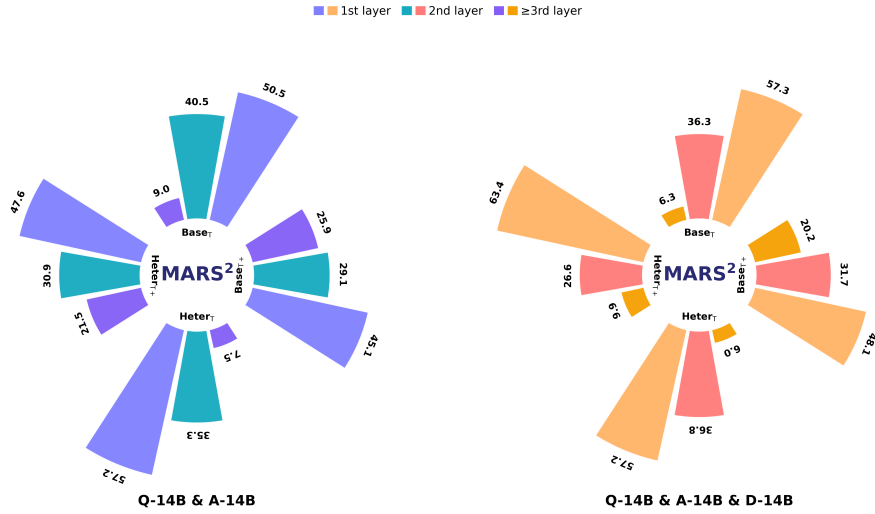


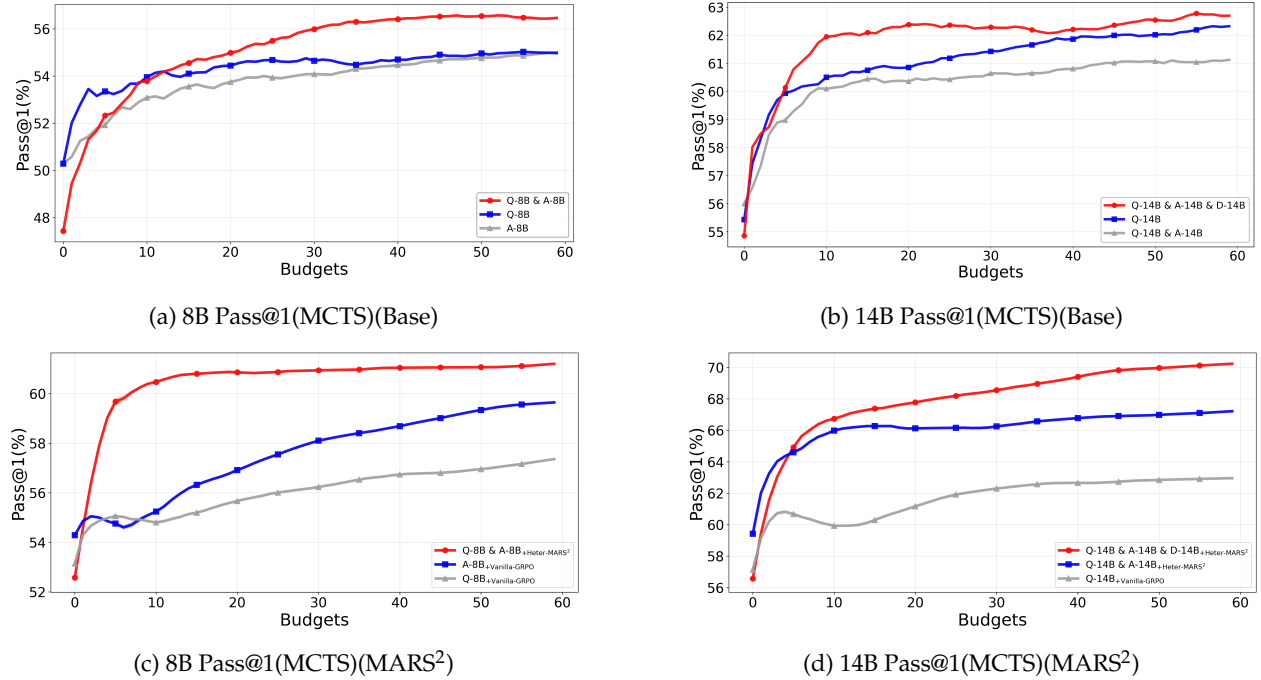
Figure 9: Node depth distributions of Qwen3-14B & AReaL-14B & DeepCoder-14B before and after training

Takeaway

- (1) **MARS²-T+ fundamentally breaks the ceiling imposed by Vanilla TTS.** MARS²-T+ upgrades test-time search into a feedback-enhanced, depth-guided, and evaluation-driven reasoning process, overcoming the core structural limits of Vanilla TTS and enabling performance beyond the previous ceiling.
- (1) **MARS² training and MARS²-T+ form a mutually reinforcing reasoning ecosystem.** MARS² training establishes structured agent collaboration, and MARS²-T+ amplifies and deepens this coordination during inference; by jointly enhancing collaborative reasoning, they produce pronounced non-linear system-level gains.
- (3) **The components of MARS²-T+ constitute a co-evolving triad rather than isolated techniques.** Error feedback improves correction, depth guidance drives exploration, and the reward model stabilizes decisions. Their coordinated interaction—from information augmentation → reasoning guidance → decision optimization—is indispensable, and MARS²-T+ reaches maximal benefit only when all three operate together.

Effectiveness of MARS²-T+. To address these limitations, we introduce MARS² and conduct a comprehensive set of experiments to evaluate the effectiveness of our improvements. Across all 8B-scale model configurations, MARS²-T+ consistently outperforms Vanilla TTS. For instance, with Qwen3-8B (Table 1), replacing Vanilla TTS with MARS²-T+—while keeping model parameters unchanged—raises Pass@1(MCTS) from 54.3% to 57.7% and PASS@N from 68.6% to 71.4%. This indicates that, under the same compute budget, MARS²-T+ not only increases the likelihood of producing correct solutions but also yields more stable and higher-quality candidate sets. Unlike Vanilla TTS, which relies solely on sparse public test cases and therefore provides limited guidance, MARS²-T+ more effectively leverages intermediate refinement signals and final-stage evaluations, directing computational resources toward more promising search branches and ultimately improving budget utilization efficiency.

Synergistic Effects Between MARS² Training and MARS²-T+ Inference Enhancement. We further examine how MARS² training interacts with T+ inference by comparing multi-agent configurations before and after training. The results show that MARS²-T+ brings only modest gains on Base multi-model systems—for example, Qwen3-8B + AReaL-8B improves only marginally under MARS²-T+. In contrast, once the same model pair is trained with MARS², MARS²-T+ unlocks substantially higher performance, pushing the Pass@1(MCTS) score to 62.9%, a level unattainable by any Base multi-agent configuration even with increased inference budgets(Table 1). This contrast highlights that MARS² training reshapes the collaborative policy landscape across agents, enabling MARS²-T+ to exploit deeper refinement opportunities and achieve performance ceilings that Vanilla TTS and Base model cannot reach. From the perspective of scalability, the multi-agent TTS behavior before and after training diverges even more clearly: in the Base setting, heteroge-


Figure 10: System-level performance before (top) and after (bottom) training with MARS².

neous model combinations do not consistently outperform homogeneous shared-parameter ones, and in some 14B configurations they even underperform (Figure 10b), suggesting that Vanilla TTS fails to convert policy heterogeneity into effective cooperative gains. After MARS² training, however, all model combinations exhibit a pronounced multi-agent scaling trend—performance steadily increases and becomes more stable as the number or heterogeneity of participating agents grows. This shift demonstrates that MARS² training not only improves single-sample quality but also reshapes collaborative strategy structures, enabling MARS²-T+ to operate within a more compatible policy space and realize deeper reasoning expansion. Together, the two stages form a mutually reinforcing capability loop, raising both the performance ceiling and the scalability of LLMs on complex code-generation tasks.

Table 1: Performance comparison between Vanilla TTS and MARS²-T+(w/ RM and w/ all).

Methods	Pass@1(MCTS)			PASS@N		
	Vanilla TTS	w/ RM	w/ all	Vanilla TTS	w/ RM	w/ all
Q-8B & A-8B (Base)	57.2	57.1	58.9	69.7	69.7	71.4
Q-8B & A-8B (Homo-MARS ²)	57.2	59.4	60.0	72.6	72.6	69.1
Q-8B & A-8B (Heter-MARS ²)	61.7	62.3	62.9	75.4	75.4	72.0
Q-14B & A-14B (Base)	62.9	63.4	65.1	74.9	74.9	78.9
Q-14B & A-14B (Heter-MARS ²)	68.9	68.6	70.3	79.4	79.4	80.6

Ablation on Reward Models and Their Impact on TTS Stability. As discussed earlier, rollouts during training can access the full set of test cases, whereas inference is restricted to public test cases, creating a clear mismatch in reward signals between the two stages. To quantify the impact of this mismatch on TTS, we conduct a series of Reward Model (RM) ablation studies (Table 2). In the 14B multi-agent setting, the performance of Vanilla TTS (gray) fluctuates substantially as the inference budget increases, indicating that supervision derived solely from public test cases is too sparse to provide stable guidance. Introducing a generic Skywork-Reward model (blue) reduces volatility but yields only limited performance gains. In contrast, the RM fine-tuned on training trajectories (orange) produces markedly smoother curves and consistently outperforms the other variants across all budget levels. A similar trend is observed in the 8B multi-agent configuration: although the fine-tuned RM does not always surpass Vanilla TTS under low budgets, it significantly improves output stability and gradually achieves superior performance as the budget grows. Discriminative metrics further confirm this effect: AUC-ROC improves from 73.0% to 79.3%,

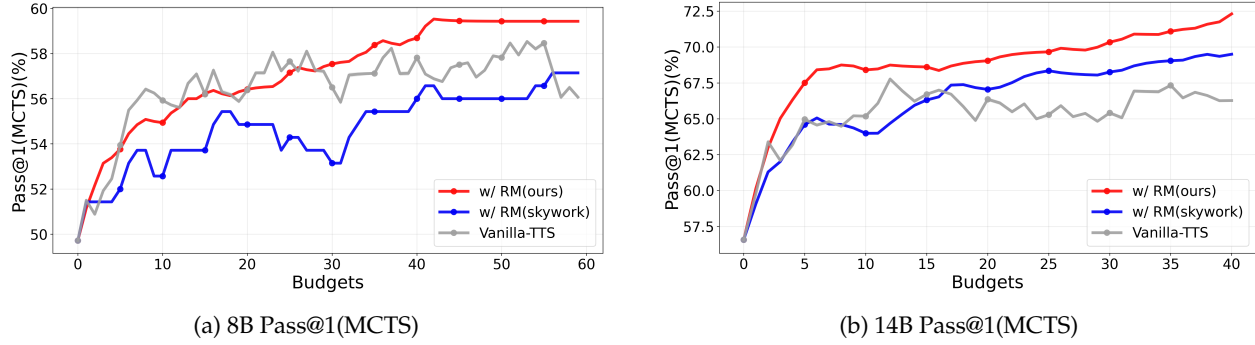


Figure 11: Ablation experiments of reward model.

and Spearman correlation increases from 39.7 to 50.6. Together with the TTS results, these findings show that a task-aligned, high-quality RM is essential for stabilizing multi-agent TTS and mitigating the reward discrepancy between training and inference, serving as a necessary component rather than an optional addition.

Table 2: Performance evaluation of Reward Models. Comparison of base vs. fine-tuned versions across Pre-train and Post-train benchmarks using Adaptive Accuracy, AUC-ROC, and Spearman correlation.

Model	Loss	Pre-train (150 nodes)			Post-train (60 nodes)		
		Adapt. Acc	AUC-ROC	Spearman	Adapt. Acc	AUC-ROC	Spearman
Skywork-Reward (Base)	-	65.5	71.2	36.7	66.3	73.0	39.7
Ours (BT Variant)	BT	62.1	67.4	30.1	61.8	66.7	28.9
Ours (MSE Variant)	MSE	69.9	78.7	49.7	71.6	79.3	50.6

Necessity of Refinement and Depth-Aware Guidance in Multi-Agent TTS. To evaluate the necessity of refinement-enhanced feedback and depth guidance in MARS²-T+, we analyze both node-depth distribution and final reasoning performance. As shown in Figure 9, Vanilla TTS exhibits a severe shallow-search bias in the 14B model series: 93.7% of nodes appear within the first two layers, while nodes at depth(≥ 4) account for fewer than 7%—a pattern that becomes even more pronounced in heterogeneous settings. After introducing refinement and depth guidance, the proportion of deeper nodes increases markedly (e.g., rising from 6.3% to 20.2%), indicating that the mechanism effectively reallocates computation toward more promising deep trajectories. The performance results further corroborate the necessity of refinement-enhanced feedback and depth guidance within the search process. When only an RM is added, candidate quality may be insufficient for reliable ranking, occasionally causing slight degradation. For example, 0.1% Pass@1(MCTS) drop in the Qwen3-8B & AReaL-8B Base configuration and 0.3% decrease in the trained Qwen3-14B & AReaL-14B (Heter-MARS²) setting (Table 1). In contrast, once refinement-enhanced feedback and depth guidance are incorporated, these regressions disappear and are replaced by consistent gains across model scales. Collectively, these findings demonstrate that refinement and depth guidance are essential for multi-agent tree search: they correct shallow-search bias, strengthen deep exploration, and enable the RM to function reliably, thereby substantially stabilizing and improving TTS performance.

4 Diversity Analysis of MARS²

4.1 Diversity Metrics

To comprehensively evaluate the algorithmic and cognitive diversity of code generated by our method, we design a multi-level, complementary evaluation framework that encompasses semantic distribution at the code level, algorithmic differences, and cognitive strategy diversity in reasoning processes. We employ pass@K to measure the method’s capability in exploring correct solutions. Average Embedding Clusters (AEC) quantifies semantic diversity among code samples. Distinct Algorithms at K (DA@K), Effective

number of Algorithms (EA) and Normalized Area Under the Diversity Curve (NAUDC) [26] directly quantify the diversity of algorithms themselves. Exploratively, we introduce the G-Vendi metric [24] to capture cognitive strategy differences in the model’s reasoning paths (CoT) and final answers through gradient space distribution. Importantly, all diversity metrics—including AEC, DA@K, EA, NAUDC, and G-Vendi—are evaluated solely on functionally correct solutions, ensuring that the measured diversity reflects meaningful algorithmic differences rather than superficial variations.

pass@K. We adopt pass@K, a widely used metric in code generation evaluation. Formally, pass@K computes the probability that among K sampled completions for a given problem, at least one passes all test cases. While pass@K primarily reflects a model’s ability to generate correct solutions, it also indirectly captures the diversity of generated code: a higher pass@K suggests broader exploration of the solution space.

Average Embedding Clusters. Embedding-based methods have been widely used for code diversity assessment. For each problem, we employ the advanced code embedding model to generate semantic vectors for the correct answers produced by the model. DBSCAN clustering [13] is then applied to group all correct answers for that problem. We use the average number of clusters to reflect the diversity of the model’s generated answers. The average numbers of clusters (AEC) is then computed as:

$$AEC = \frac{1}{|Q|} \sum_{q \in Q} C(A_q) \quad (8)$$

where Q denotes the set of evaluated problems, and $C(A_q)$ is the numbers of clusters obtained from the correct solution set A_q from problem q . A higher AEC suggests that the model produces functionally correct solutions that are more widely dispersed in the semantic space, hence exhibiting higher semantic diversity.

DA@K, EA, NAUDC. Following the setup in [26], we adopt DA@K, EA, and NAUDC to comprehensively assess the algorithmic diversity of code generated by models from multiple perspectives. We use a LLM to determine whether two code solutions implement the same algorithm, facilitating the clustering of correct answer sets. We calculate the following metrics:

DA@K measures the average number of distinct algorithms covered when sampling K solutions from the solution set. Let M denote the number of algorithmic clusters and s_m the size of the m -th cluster in a solution set of total size N . It is calculated as

$$DA@K = \sum_{m=1}^M \left(1 - \frac{\binom{N-s_m}{K}}{\binom{N}{K}} \right) \quad (9)$$

EA characterizes the distribution of solution strategies across clusters. Let $p_m = \frac{s_m}{N}$ be the empirical probability of generating a solution from cluster m . It is defined as

$$EA = \exp \left(- \sum_{m=1}^M p_m \ln p_m \right) \quad (10)$$

NAUDC integrates DA@K over varying sampling budgets to assess the average diversity across solution set sizes. Denoting the maximum evaluation budget as K_{max} , we compute

$$NAUDC = \frac{1}{K_{max} - 1} \sum_{k=1}^{K_{max}} DA@k \quad (11)$$

G-Vendi. Previous metrics primarily focus on code-level diversity. We adopt the G-Vendi [24] metric to assess diversity across both the reasoning process and the generated code. G-Vendi captures diversity at the level of cognitive strategies by examining how samples are distributed in the loss-gradient space of a small proxy model. We compute the loss gradient of each sample using a lightweight proxy model, where x denotes the code problem and y denotes the combined chain-of-thought (CoT) reasoning and final answer:

$$g_\theta(x, y) = -\nabla \log P(y | x; \theta) \quad (12)$$

We then normalize the gradients and apply a random projection for dimensionality reduction. We then construct a covariance matrix from the projected gradients and compute the Shannon entropy of its eigenvalue distribution. Specifically, let $\{\lambda_i^K\}$ denote the normalized eigenvalues of the covariance matrix K , which form a probability distribution over gradient variation modes. The G-Vendi score is defined as the exponential of this entropy:

$$\text{G-Vendi}(D) = \exp \left(- \sum_i \lambda_i^K \log \lambda_i^K \right) \quad (13)$$

Experimental Setup. We evaluate the code generation diversity of baseline methods and our proposed approach on the LiveCodeBench v6 dataset. We retain only those tasks for which all methods being compared can generate at least one functionally correct solution, in order to eliminate the confounding effects of differences in functional correctness among methods on the diversity assessment and ensure that the observed diversity differences purely reflect the inherent characteristics of the methods themselves. This filtering results in a total of 95 tasks, which constitute our evaluation subset.

We employ `jina-code-embeddings-1.5b`[25] as the advanced code embedding model. **Qwen2.5-7B-Instruct** (with temperature set to 0) is used to determine whether two code solutions implement the same algorithm, enabling the clustering required for calculating metrics such as $DA@K$ and EA . For $DA@K$, we select $K = 20$ to reflect the diversity of code generated by the models. For NAUADC, we set $K_{max} = 60$ to cover the range of all correct solutions generated per problem. For G-Vendi, we use **Qwen2.5-0.5B-Instruct** to compute the loss gradient.

4.2 Diversity Evaluation

Takeaway

- (1) **Heterogeneous multi-agent collaboration substantially enhances performance and solution-space exploration capability.** Heter-MARS² achieves the highest pass@K scores across both 8B (75.4%) and 14B (81.7%) model scales, significantly outperforming baseline methods. This demonstrates its superior ability to expand the exploration of high-quality regions within the underlying solution space.
- (2) **System-level diversity consistently increases with both the number of agents and architectural heterogeneity.** Both scaling the number of models and adopting heterogeneous architectures lead to consistent improvements in algorithmic diversity and distributional uniformity. This indicates that the multi-agent paradigm not only broadens the policy space but also mitigates over-reliance on any single solution trajectory.
- (3) **Multi-agent collaboration effectively expands the cognitive strategy space.** The G-Vendi score exhibits a systematic positive correlation with the number of collaborating agents. This confirms that the multi-agent framework fosters greater diversity not only at the code level but also in high-level cognitive reasoning strategies.

We computed diversity metrics for the code generated by the baseline methods and our proposed approach. The results, summarized in Table 3, reveal several key insights:

Heter-MARS² achieves the highest pass@K scores within both the 8B and 14B model families. Specifically, in the 8B model family, Heter-MARS² attains a pass@K of 75.4%, and in the 14B model family, Heter-MARS² (2-model) achieves a pass@K of 81.7%—significantly outperforming the baseline methods. These results demonstrate that our proposed approach effectively enhances the model’s capacity to explore the underlying solution space, which, to some extent, reflects an improvement in the diversity of the generated code.

Algorithmic diversity and distributional uniformity improve as the number of models increases. This trend is confirmed in Table 3 vanilla TTS result (14B), where NAUADC rises from 1.659 to 1.962, and is further enhanced by our approach: in the 8B model family, multi-agent collaboration (MA-2model) increases DA@K from 1.554 (SA-1model) to 1.677 and raises NAUADC to 1.750. The concurrent improvement in the EA metric—e.g., reaching 1.544 for 14B Heter-MARS²—demonstrates that the multi-agent mechanism not

only expands the policy space but also effectively promotes more uniform algorithmic distributions, thereby mitigating over-reliance on a single solution path.

Table 3: Performance and diversity comparison of different methods on 8B and 14B models.

Method	pass@K	AEC	DA@K	EA	NAUADC	G-Vendi
8B Model						
Vanilla-TTS						
Q-8B	68.6	1.053	1.631	1.332	1.670	6.688
A-8B	66.9	1.052	1.641	1.348	1.682	6.946
Q-8B & A-8B	72.0	1.295	1.634	1.321	1.686	7.146
Vanilla-GRPO						
Q-8B	73.7	1.274	1.733	1.375	1.787	6.690
A-8B	69.1	1.116	1.625	1.350	1.673	6.799
Q-8B & A-8B	72.0	1.190	1.645	1.333	1.707	7.063
Homo-MARS²						
Q-8B	71.4	1.463	1.554	1.271	1.618	5.962
A-8B	69.7	1.052	1.608	1.307	1.658	6.564
Q-8B & A-8B	72.6	1.315	1.664	1.341	1.716	6.403
Heter-MARS²						
Q-8B & A-8B	75.4	1.431	1.677	1.348	1.750	6.901
14B Model						
Vanilla-TTS						
Q-14B	77.7	1.032	1.517	1.261	1.575	7.666
A-14B	75.4	1.000	1.594	1.320	1.659	6.908
D-14B	68.0	1.042	1.712	1.406	1.759	7.392
Q-14B & A-14B	79.4	1.095	1.698	1.375	1.766	7.668
Q-14B & A-14B & D-14B	79.4	1.231	1.882	1.478	1.962	8.808
Vanilla-GRPO						
Q-14B	77.1	1.095	1.703	1.369	1.755	6.344
A-14B	76.0	1.063	1.705	1.405	1.753	5.970
D-14B	73.7	1.200	1.788	1.441	1.840	7.897
Q-14B & A-14B	78.9	1.179	1.836	1.448	1.939	6.534
Q-14B & A-14B & D-14B	79.4	1.147	1.852	1.464	1.919	8.032
Homo-MARS²						
Q-14B	78.9	1.073	1.595	1.300	1.644	7.324
A-14B	81.1	1.084	1.685	1.358	1.757	6.335
D-14B	70.9	1.168	1.692	1.373	1.739	8.335
Q-14B & A-14B	79.4	1.042	1.687	1.367	1.749	7.250
Q-14B & A-14B & D-14B	78.9	1.147	1.837	1.445	1.889	8.750
Heter-MARS²						
Q-14B & A-14B	81.7	1.042	1.712	1.369	1.793	6.980
Q-14B & A-14B & D-14B	80.0	1.116	1.941	1.544	2.033	8.719

Heter-MARS² demonstrates superior capability in enhancing algorithmic diversity compared to Homo-MARS². At the 8B model scale, Heter-MARS² consistently outperforms Homo-MARS² under equivalent model-count configurations, achieving a DA@K of 1.677 and an NAUADC of 1.750—improvements of 0.013 and 0.034, respectively, over the SA baseline. This advantage is further validated and amplified at the 14B scale, where NAUADC increases significantly from 1.749 (SA) to 1.793 (Heter-MARS²). These results indicate that the joint training mechanism employed by Heter-MARS² effectively overcomes the limitations of independent training, enabling the models to explore a broader algorithmic space and thereby substantially expanding the solution space.

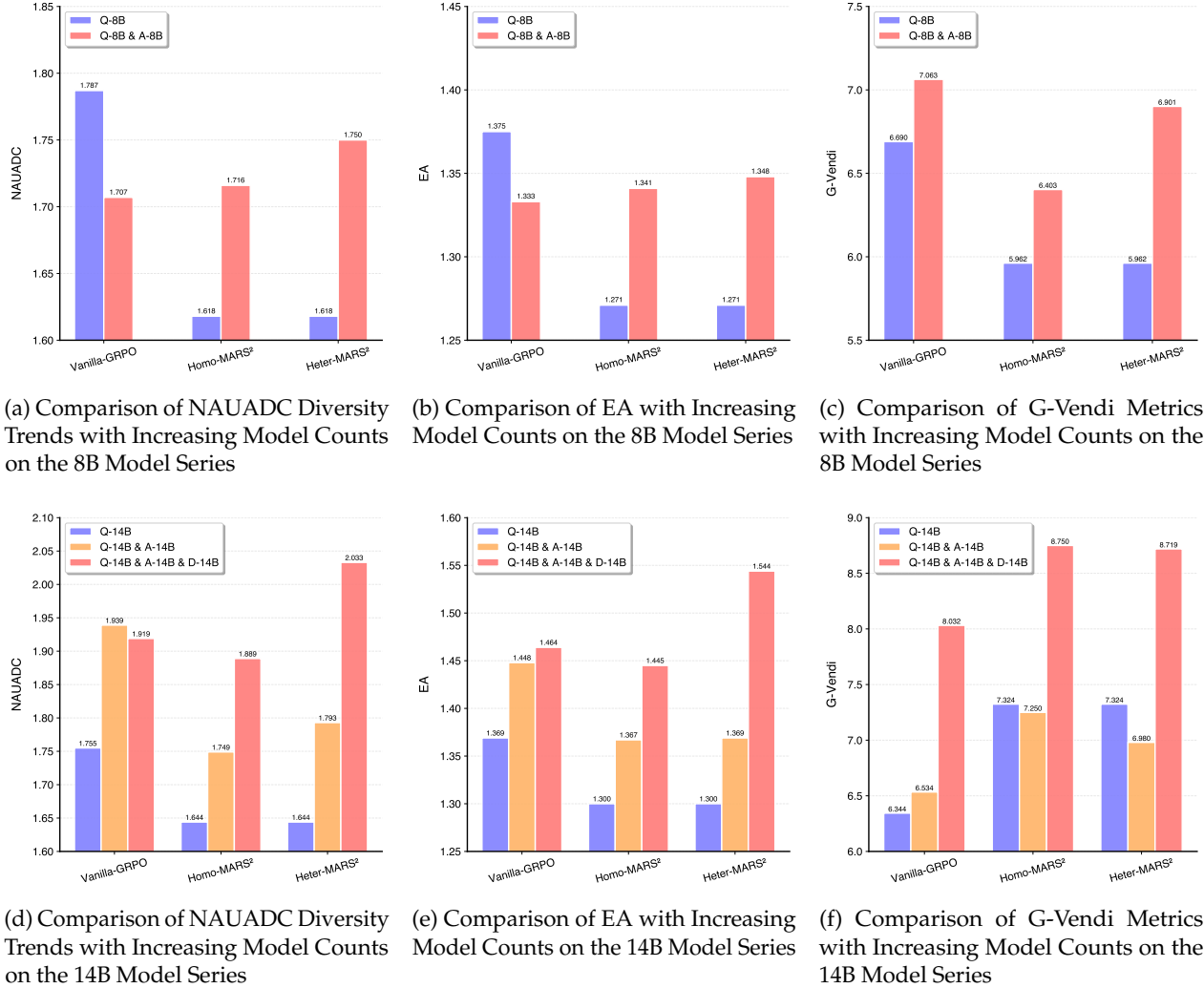


Figure 12: Analysis of Diversity metrics Trends with Increasing Model Counts across 8B and 14B Model Series.

Multi-agent collaboration expands the cognitive strategy space. Consistent with the trends observed in code-level diversity metrics (DA@K and NAUADC), the G-Vendi score exhibits a positive correlation with the number of models. This trend is particularly pronounced in the 8B model family, and in the 14B model family, all methods show significant gains when transitioning from a single-model baseline to three-model collaboration. We provide additional diversity analyses of the TTS-enhanced method in Appendix D.

5 Preliminary

5.1 GRPO

GRPO (Group Relative Policy Optimization), a reinforcement learning algorithm introduced by DeepSeekMath[49], eliminates the need for the critic model used in PPO [48]. Its core idea is to leverage relative rewards within a group of outputs to estimate advantages. Specifically, it uses the average reward of multiple outputs sampled from the same prompt as a baseline for reward normalization. This achieves a critic-free training paradigm, which effectively reduces the computational cost of training.

Given a prompt p , a set of outputs $\{o_1, o_2, \dots, o_G\}$ is sampled from the old policy model $\pi_{\theta_{old}}$, where G represents the group size. Each output o_i receives a scalar reward r_i through a reward model or environment feedback. To compute the advantage, the rewards for the group are normalized by applying a z-score, with

the advantage of all tokens set to the normalized reward:

$$\hat{A}_{i,t} = \frac{r_i - \text{mean}(r_1, r_2, \dots, r_G)}{\text{std}(r_1, r_2, \dots, r_G)} \quad (14)$$

The policy π_θ is updated by maximizing the following objective to increase the probability of generating responses with positive relative advantages:

$$\begin{aligned} \mathcal{J}_{GRPO}(\theta) = \mathbb{E}[q \sim P(Q), \{o_i\}_{i=1}^G \sim \pi_{\theta_{old}}(O|q)] \\ \frac{1}{G} \sum_{i=1}^G \frac{1}{|o_i|} \sum_{t=1}^{|o_i|} \left\{ \min \left[\frac{\pi_\theta(o_{i,t}|q, o_{i,<t})}{\pi_{\theta_{old}}(o_{i,t}|q, o_{i,<t})} \hat{A}_{i,t}, \text{clip} \left(\frac{\pi_\theta(o_{i,t}|q, o_{i,<t})}{\pi_{\theta_{old}}(o_{i,t}|q, o_{i,<t})}, 1 - \epsilon, 1 + \epsilon \right) \hat{A}_{i,t} \right] - \beta \mathbb{D}_{KL}(\pi_\theta || \pi_{ref}) \right\} \end{aligned} \quad (15)$$

where $\mathbb{D}_{KL}(\pi_\theta || \pi_{ref})$ measures the divergence between the current and reference policies, and β controls this regularization strength for stable policy updates.

5.2 AB-MCTS

AB-MCTS (Adaptive Branching Monte Carlo Tree Search) is an inference-time computation framework designed to scale LLM reasoning[19]. It acts as a unified strategy, combining the parallel output diversity of repeated sampling with the multi-turn solution refinement of sequential methods. This approach implements an adaptive MCTS that achieves dynamic control over search depth and width.

The framework is designed to utilize a set of m heterogeneous or Homogeneous agents (LLMs), denoted as $\{\mathcal{A}_j\}_{j=1}^m$. To effectively capture the local performance context of each agent, we adopt the *Multiple GEN Nodes* strategy, in which every search node conceptually maintains a distinct GEN node for each agent \mathcal{A}_j , allowing independent tracking of their exploration potential. The action space for each agent \mathcal{A}_j is simplified into two distinct meta-actions through node aggregation:

- **GEN (Go Wider):** Represents exploration by generating a new candidate answer, expanding the search width.
- **CON (Go Deeper):** Represents exploitation by refining an existing solution derived from a child node.

The overall selection process operates hierarchically:

- **Model Selection:** The primary decision of which agent to utilize is formulated as a Multi-Armed Bandit (MAB) problem. Thompson Sampling is applied to the aggregated performance statistics of all agents to select the agent \mathcal{A}_{j^*} with the highest current potential for the expansion step.
- **Node Selection:** Once the agent \mathcal{A}_{j^*} is determined, a secondary decision is made within its specific sub-tree. This choice between exploration (GEN) and exploitation (CON) is modeled as a binary bandit problem. Thompson Sampling is used again to choose the specific best action associated with the selected agent \mathcal{A}_{j^*} .

For normalized scores $r \in [0, 1]$, the posterior distribution of the expected score for each action $a \in \{\text{GEN, CON}\}$ is modeled as a Beta distribution $\text{Beta}(\alpha_a, \beta_a)$. The parameters are updated using the history of observed scores $\mathcal{D}_a = \{r_1, \dots, r_K\}$ associated with that action:

$$\alpha_a = \tilde{\alpha} + \sum_{k=1}^K r_k, \quad \beta_a = \tilde{\beta} + \sum_{k=1}^K (1 - r_k) \quad (16)$$

where $\tilde{\alpha}$ and $\tilde{\beta}$ are prior hyperparameters.

This heterogeneous multi-agent framework naturally accommodates the homogeneous multi-role scenario: when the system contains only one agent ($m = 1$) with different roles, the Model Selection step automatically selects that agent, and the search relies solely on the Node Selection step to adaptively balance exploration (GEN) and exploitation (CON).

6 Related Works

6.1 Reinforcement Learning

Recent progress in reinforcement learning has efficiently strengthened reasoning and alignment capabilities of LLM by facilitating policy optimization[71, 34, 67].

6.1.1 Reinforcement Learning for LLM

Several representative methods, such as PPO[48] and VC-PPO[65], rely on explicit value estimation to provide stable training dynamics. While value-free methods including GRPO[49], Dr.GRPO[38], DAPO[64] and GSPO[73] reduce dependence on critic models and yield more scalable optimization. Preference optimization-based methods, such as DPO[47], Focused-DPO[69] and Selective DPO[15], further simplify the learning pipeline by aligning models directly with preference data, bypassing reward modeling altogether. These methods collectively provide diverse optimization pathways for LLM training, advancing model performance.

6.1.2 Multi-Agent Reinforcement Learning

Whereas supervised fine-tuning excel at enhancing individual LLMs but cannot effectively capture emergent multi-agent dynamics (e.g., long-horizon coordination, role specialization, and credit assignment), reinforcement learning has been increasingly employed to directly optimize collaborative policies in LLM-based multi-agent systems, targeting sustained improvements in collective performance [51, 29]. A common paradigm uses external validator scores as reward signals to jointly fine-tune multiple agents, as demonstrated by MAPoRL [45]. To better handle agent heterogeneity and training instability, subsequent works incorporate group-aware optimization and stability mechanisms. JoyAgents-R1 [17] combines GRPO with marginal-benefit selection and adaptive memory to enable stable co-evolution of diverse agents. MAGRPO [37] further introduces a centralized group advantage function that explicitly optimizes joint policies for cooperative tasks. For large-scale systems with highly specialized agents, MarsRL [36] proposes agentic pipeline parallelism paired with agent-specific rewards, achieving significant reasoning gains in open-source multi-agent settings. Together, these methods mark a clear evolution from basic shared-reward fine-tuning to group-level and scalable policy optimization.

6.2 Test-Time Scaling

Test-Time Scaling (TTS) has emerged as a compelling, training-agnostic methodology for augmenting the performance of LLMs by judiciously increasing the computational budget during the inference phase[57, 70]. In this section, test-time scaling is categorized based on the paradigms of single-agent and multi-agent systems.

6.2.1 Single-Agent

Parallel Scaling is a common test-time scaling method[70], in which a single LLM-based agent generates multiple candidate responses to the same query, followed by an aggregation mechanism that selects or refines the final output. One of the most widely studied methods is Best-of-N[50] strategy, where N independent samples are generated, and the one with the highest likelihood or score is selected. Another common aggregation method is Majority Voting[3, 54, 43], which selects the most frequently generated answer across multiple reasoning paths. Another prominent method is Sequential Scaling[70], which explicitly directs the LLM-based agent to perform iterative computations based on intermediate steps. Chain-of-Thought (CoT)[55, 30, 6, 21] prompts the model to generate detailed, step-by-step reasoning trajectory. Building upon this, researchers have proposed hybrid scaling methods[57, 70] combining the complementary benefits of parallel and sequential scaling, such as Tree-of-Thoughts (ToT)[62], Graph-of-Thoughts (GoT)[2, 63], and Monte Carlo Tree Search (MCTS)-based reasoning methods[58, 74]. They significantly enhance the LLM’s reasoning capabilities by exploring a wider search space.

6.2.2 Multi-Agent

Single-agent test-time scaling focuses on exploring diverse reasoning paths within a single model to expand the search space. In contrast, multi-agent test-time scaling leverages structured collaboration among agents, integrating their complementary advantages to effectively overcome the inherent limitations and intrinsic biases of single-agent systems[52]. A prominent avenue within multi-agent test-time scaling focuses on consensus. The seminal Multi-Agent Debate framework [31, 5, 11] establishes a debate-centric structure to promote divergent ideation, wherein multiple agents engage in a reciprocal “tit-for-tat” dialogue under the supervision of an adjudicator.

A second critical method involves structured search. [19] introduces Adaptive Branching Monte Carlo Tree Search (AB-MCTS), which leverages multi-agent collaboration for test-time scaling by unifying distributed exploration of solution spaces and collective feedback-driven exploitation. Structured planning is another focus. Frameworks such as Chain-of-Agents[28] and PlanGEN[46] concentrate on the generation of intricate planning and reasoning trajectories via multi-agent collaboration. The integration of external tools has also been a focus, exemplified by TUMIX[10], which employs a heterogeneous mixture of tool-use strategies. This paradigm has been successfully applied to specialized domains, including METAL[27] for chart generation and Multi²[4] for multi-document processing.

7 Conclusion

In this work, we propose and address a critical bottleneck in leveraging multi-agent systems for complex reasoning: the disconnect between test-time scaling and pre-deployment coordination training. To bridge this gap, we proposed MARTI-MARS², a novel multi-agent reinforced training and inference framework based on self-search scaling. By modeling the agents’ collaborative exploration process as a dynamic and learnable environment, our framework enables a pivotal evolution from single-agent baselines to parameter-sharing homogeneous multi-role paradigms, and ultimately to heterogeneous multi-agent paradigms. Extensive experiments on challenging code generation benchmarks across various model scales demonstrate that MARTI-MARS² significantly enhances reasoning performance: with two collaborating 32B models achieving 77.7% which surpasses strong proprietary baselines like O4-Mini(High). Besides, we unveil a new dimension of multi-agent scaling laws: the progressive shift towards homogeneous multi-role and heterogeneous multi-agent collaboration yields higher reinforcement learning performance ceilings, more robust test-time scaling capabilities, and greater policy diversity. These findings provide a scalable and effective pathway for advancing LLMs reasoning through multi-agent coordination.

While MARTI-MARS² has demonstrated the power of multi-agent systems in code generation, we believe that our framework serves as a foundational step toward uncovering what multi-agent scaling laws can truly achieve. The current generation of benchmarks, although challenging, often consists of isolated reasoning problems that may not fully exploit the emergent capabilities of large-scale agent coordination. To discover the next phase of multi-agent scaling laws, future research should pivot towards more promising tasks, such as those within enterprise or organizational scenarios.

8 Acknowledgements

This work is supported by the Shanghai Municipal Science and Technology Major Project.

References

- [1] Wasi Uddin Ahmad, Sean Narendhiran, Somshubra Majumdar, Aleksander Ficek, Siddhartha Jain, Jocelyn Huang, Vahid Noroozi, and Boris Ginsburg. Opencodereasoning: Advancing data distillation for competitive coding. *arXiv preprint arXiv:2504.01943*, 2025.
- [2] Maciej Besta, Nils Blach, Ales Kubicek, Robert Gerstenberger, Michal Podstawski, Lukas Gianinazzi, Joanna Gajda, Tomasz Lehmann, Hubert Niewiadomski, Piotr Nyczek, et al. Graph of thoughts: Solving elaborate problems with large language models. In *Proceedings of the AAAI conference on artificial intelligence*, volume 38, pages 17682–17690, 2024.
- [3] Bradley Brown, Jordan Juravsky, Ryan Ehrlich, Ronald Clark, Quoc V Le, Christopher Ré, and Azalia Mirhoseini. Large language monkeys: Scaling inference compute with repeated sampling. *arXiv preprint arXiv:2407.21787*, 2024.
- [4] Juntai Cao, Xiang Zhang, Raymond Li, Jiaqi Wei, Chuyuan Li, Shafiq Joty, and Giuseppe Carenini. Multi2: Multi-agent test-time scalable framework for multi-document processing. In *Proceedings of The 5th New Frontiers in Summarization Workshop*, pages 135–156, 2025.
- [5] Chi-Min Chan, Weize Chen, Yusheng Su, Jianxuan Yu, Wei Xue, Shanghang Zhang, Jie Fu, and Zhiyuan Liu. Chateval: Towards better llm-based evaluators through multi-agent debate. *arXiv preprint arXiv:2308.07201*, 2023.
- [6] Qiguang Chen, Libo Qin, Jinhao Liu, Dengyun Peng, Jiannan Guan, Peng Wang, Mengkang Hu, Yuhang Zhou, Te Gao, and Wanxiang Che. Towards reasoning era: A survey of long chain-of-thought for reasoning large language models. *arXiv preprint arXiv:2503.09567*, 2025.
- [7] Yiqun Chen, Lingyong Yan, Weiwei Sun, Xinyu Ma, Yi Zhang, Shuaiqiang Wang, Dawei Yin, Yiming Yang, and Jiaxin Mao. Improving retrieval-augmented generation through multi-agent reinforcement learning. *arXiv preprint arXiv:2501.15228*, 2025.
- [8] Yiqun Chen, Erhan Zhang, Lingyong Yan, Shuaiqiang Wang, Jizhou Huang, Dawei Yin, and Jiaxin Mao. Mao-arag: Multi-agent orchestration for adaptive retrieval-augmented generation. *arXiv preprint arXiv:2508.01005*, 2025.
- [9] Yiqun Chen, Lingyong Yan, Zixuan Yang, Erhan Zhang, Jiashu Zhao, Shuaiqiang Wang, Dawei Yin, and Jiaxin Mao. Beyond monolithic architectures: A multi-agent search and knowledge optimization framework for agentic search. *arXiv preprint arXiv:2601.04703*, 2026.
- [10] Yongchao Chen, Jiefeng Chen, Rui Meng, Ji Yin, Na Li, Chuchu Fan, Chi Wang, Tomas Pfister, and Jinsung Yoon. Tumix: Multi-agent test-time scaling with tool-use mixture. *arXiv preprint arXiv:2510.01279*, 2025.
- [11] Steffi Chern, Zhen Fan, and Andy Liu. Combating adversarial attacks with multi-agent debate. *arXiv preprint arXiv:2401.05998*, 2024.
- [12] Ahmed El-Kishky, Alexander Wei, Andre Saraiva, Borys Minaiev, Daniel Selsam, David Dohan, Francis Song, Hunter Lightman, Ignasi Clavera, Jakub Pachocki, et al. Competitive programming with large reasoning models. *arXiv preprint arXiv:2502.06807*, 2025.
- [13] Martin Ester, Hans-Peter Kriegel, Jörg Sander, Xiaowei Xu, et al. A density-based algorithm for discovering clusters in large spatial databases with noise. In *kdd*, volume 96, pages 226–231, 1996.
- [14] Wei Fu, Jiaxuan Gao, Xujie Shen, Chen Zhu, Zhiyu Mei, Chuyi He, Shusheng Xu, Guo Wei, Jun Mei, Jiashu Wang, et al. Areal: A large-scale asynchronous reinforcement learning system for language reasoning, 2025.
- [15] Chengqian Gao, Haonan Li, Liu Liu, Zeke Xie, Peilin Zhao, and Zhiqiang Xu. Principled data selection for alignment: The hidden risks of difficult examples. *arXiv preprint arXiv:2502.09650*, 2025.
- [16] Daya Guo, Dejian Yang, Haowei Zhang, Junxiao Song, Ruoyu Zhang, Runxin Xu, Qihao Zhu, Shirong Ma, Peiyi Wang, Xiao Bi, et al. Deepseek-r1: Incentivizing reasoning capability in llms via reinforcement learning. *arXiv preprint arXiv:2501.12948*, 2025.
- [17] Ai Han, Junxing Hu, Pu Wei, Zhiqian Zhang, Yuhang Guo, Jiawei Lu, and Zicheng Zhang. Joyagents-r1: Joint evolution dynamics for versatile multi-llm agents with reinforcement learning. *arXiv preprint arXiv:2506.19846*, 2025.
- [18] Sirui Hong, Mingchen Zhuge, Jiaqi Chen, Xiawu Zheng, Yuheng Cheng, Ceyao Zhang, Jinlin Wang, Zili Wang, Steven Ka Shing Yau, Zijuan Lin, Liyang Zhou, Chenyu Ran, Lingfeng Xiao, Chenglin Wu, and Jürgen Schmidhuber. Metagpt: Meta programming for a multi-agent collaborative framework, 2024. URL <https://arxiv.org/abs/2308.00352>.
- [19] Yuichi Inoue, Kou Misaki, Yuki Imajuku, So Kuroki, Taishi Nakamura, and Takuya Akiba. Wider or deeper? scaling llm inference-time compute with adaptive branching tree search. *arXiv preprint arXiv:2503.04412*, 2025.

[20] Naman Jain, King Han, Alex Gu, Wen-Ding Li, Fanjia Yan, Tianjun Zhang, Sida Wang, Armando Solar-Lezama, Koushik Sen, and Ion Stoica. Livecodebench: Holistic and contamination free evaluation of large language models for code. *arXiv preprint arXiv:2403.07974*, 2024.

[21] Yixin Ji, Juntao Li, Hai Ye, Kaixin Wu, Jia Xu, Linjian Mo, and Min Zhang. Test-time computing: from system-1 thinking to system-2 thinking. *arXiv e-prints*, pages arXiv–2501, 2025.

[22] Can Jin, Hongwu Peng, Qixin Zhang, Yujin Tang, Dimitris N Metaxas, and Tong Che. Two heads are better than one: Test-time scaling of multi-agent collaborative reasoning. *arXiv preprint arXiv:2504.09772*, 2025.

[23] Can Jin, Yang Zhou, Qixin Zhang, Hongwu Peng, Di Zhang, Marco Pavone, Ligong Han, Zhang-Wei Hong, Tong Che, and Dimitris N Metaxas. Your reward function for rl is your best prm for search: Unifying rl and search-based tts. *arXiv preprint arXiv:2508.14313*, 2025.

[24] Jaehun Jung, Seungju Han, Ximing Lu, Skyler Hallinan, David Acuna, Shrimai Prabhumoye, Mostafa Patwary, Mohammad Shoeybi, Bryan Catanzaro, and Yejin Choi. Prismatic synthesis: Gradient-based data diversification boosts generalization in llm reasoning. *arXiv preprint arXiv:2505.20161*, 2025.

[25] Daria Kryvosheieva, Saba Sturua, Michael Günther, Scott Martens, and Han Xiao. Efficient code embeddings from code generation models. *arXiv preprint arXiv:2508.21290*, 2025.

[26] Seonghyeon Lee, HeeJae Chon, Joonwon Jang, Dongha Lee, and Hwanjo Yu. How diversely can language models solve problems? exploring the algorithmic diversity of model-generated code. In Christos Christodoulopoulos, Tanmoy Chakraborty, Carolyn Rose, and Violet Peng, editors, *Findings of the Association for Computational Linguistics: EMNLP 2025*, Suzhou, China, November 2025. Association for Computational Linguistics. ISBN 979-8-89176-335-7.

[27] Bingxuan Li, Yiwei Wang, Jiuxiang Gu, Kai-Wei Chang, and Nanyun Peng. Metal: A multi-agent framework for chart generation with test-time scaling. *arXiv preprint arXiv:2502.17651*, 2025.

[28] Weizhen Li, Jianbo Lin, Zhusong Jiang, Jingyi Cao, Xinpeng Liu, Jiayu Zhang, Zhenqiang Huang, Qianben Chen, Weichen Sun, Qixiang Wang, et al. Chain-of-agents: End-to-end agent foundation models via multi-agent distillation and agentic rl. *arXiv preprint arXiv:2508.13167*, 2025.

[29] Xinyi Li, Sai Wang, Siqi Zeng, Yu Wu, and Yi Yang. A survey on llm-based multi-agent systems: workflow, infrastructure, and challenges. *Vicinagearth*, 1(1):9, 2024.

[30] Zhong-Zhi Li, Duzhen Zhang, Ming-Liang Zhang, Jiaxin Zhang, Zengyan Liu, Yuxuan Yao, Haotian Xu, Junhao Zheng, Pei-Jie Wang, Xiuyi Chen, et al. From system 1 to system 2: A survey of reasoning large language models. *arXiv preprint arXiv:2502.17419*, 2025.

[31] Tian Liang, Zhiwei He, Wenxiang Jiao, Xing Wang, Yan Wang, Rui Wang, Yujiu Yang, Shuming Shi, and Zhaopeng Tu. Encouraging divergent thinking in large language models through multi-agent debate. In *Proceedings of the 2024 conference on empirical methods in natural language processing*, pages 17889–17904, 2024.

[32] Junwei Liao, Muning Wen, Jun Wang, and Weinan Zhang. Marft: Multi-agent reinforcement fine-tuning. *arXiv preprint arXiv:2504.16129*, 2025.

[33] Chris Yuhao Liu, Liang Zeng, Yuzhen Xiao, Jujie He, Jiacai Liu, Chaojie Wang, Rui Yan, Wei Shen, Fuxiang Zhang, Jiacheng Xu, et al. Skywork-reward-v2: Scaling preference data curation via human-ai synergy. *arXiv preprint arXiv:2507.01352*, 2025.

[34] Keliang Liu, Dingkang Yang, Ziyun Qian, Weijie Yin, Yuchi Wang, Hongsheng Li, Jun Liu, Peng Zhai, Yang Liu, and Lihua Zhang. Reinforcement learning meets large language models: A survey of advancements and applications across the llm lifecycle. *arXiv preprint arXiv:2509.16679*, 2025.

[35] Runze Liu, Junqi Gao, Jian Zhao, Kaiyan Zhang, Xiu Li, Biqing Qi, Wanli Ouyang, and Bowen Zhou. Can 1b llm surpass 405b llm? rethinking compute-optimal test-time scaling. *arXiv preprint arXiv:2502.06703*, 2025.

[36] Shulin Liu, Dong Du, Tao Yang, Yang Li, and Boyu Qiu. Marsrl: Advancing multi-agent reasoning system via reinforcement learning with agentic pipeline parallelism. 2025.

[37] Shuo Liu, Tianle Chen, Zeyu Liang, Xueguang Lyu, and Christopher Amato. Llm collaboration with multi-agent reinforcement learning. *arXiv preprint arXiv:2508.04652*, 2025.

[38] Zichen Liu, Changyu Chen, Wenjun Li, Penghui Qi, Tianyu Pang, Chao Du, Wee Sun Lee, and Min Lin. Understanding r1-zero-like training: A critical perspective. *arXiv preprint arXiv:2503.20783*, 2025.

[39] Haipeng Luo, Qingfeng Sun, Can Xu, Pu Zhao, Jianguang Lou, Chongyang Tao, Xiubo Geng, Qingwei Lin, Shifeng Chen, and Dongmei Zhang. Wizardmath: Empowering mathematical reasoning for large language models via reinforced evol-instruct. *arXiv preprint arXiv:2308.09583*, 2023.

[40] Michael Luo, Sijun Tan, Roy Huang, Ameen Patel, Alpay Ariyak, Qingyang Wu, Xiaoxiang Shi, Rachel Xin, Colin Cai, Maurice Weber, et al. Deepcoder: A fully open-source 14b coder at o3-mini level. *Notion Blog*, 2025.

[41] Moonshot AI. Kimi k2.5: Visual agentic intelligence. <https://www.kimi.com/blog/kimi-k2-5.html>, 2026.

[42] Niklas Muennighoff, Zitong Yang, Weijia Shi, Xiang Lisa Li, Li Fei-Fei, Hannaneh Hajishirzi, Luke Zettlemoyer, Percy Liang, Emmanuel Candès, and Tatsunori B Hashimoto. s1: Simple test-time scaling. In *Proceedings of the 2025 Conference on Empirical Methods in Natural Language Processing*, pages 20286–20332, 2025.

[43] Alex Nguyen, Dheeraj Mekala, Chengyu Dong, and Jingbo Shang. When is the consistent prediction likely to be a correct prediction? *arXiv preprint arXiv:2407.05778*, 2024.

[44] Melissa Z Pan, Mert Cemri, Lakshya A Agrawal, Shuyi Yang, Bhavya Chopra, Rishabh Tiwari, Kurt Keutzer, Aditya Parameswaran, Kannan Ramchandran, Dan Klein, et al. Why do multiagent systems fail? In *ICLR 2025 Workshop on Building Trust in Language Models and Applications*, 2025.

[45] Chanwoo Park, Seungju Han, Xingzhi Guo, Asuman E Ozdaglar, Kaiqing Zhang, and Joo-Kyung Kim. Maporl: Multi-agent post-co-training for collaborative large language models with reinforcement learning. In *Proceedings of the 63rd Annual Meeting of the Association for Computational Linguistics (Volume 1: Long Papers)*, pages 30215–30248, 2025.

[46] Mihir Parmar, Xin Liu, Palash Goyal, Yanfei Chen, Long Le, Swaroop Mishra, Hossein Mobahi, Jindong Gu, Zifeng Wang, Hootan Nakhost, et al. Plangen: A multi-agent framework for generating planning and reasoning trajectories for complex problem solving. *arXiv preprint arXiv:2502.16111*, 2025.

[47] Rafael Rafailov, Archit Sharma, Eric Mitchell, Christopher D Manning, Stefano Ermon, and Chelsea Finn. Direct preference optimization: Your language model is secretly a reward model. *Advances in neural information processing systems*, 36:53728–53741, 2023.

[48] John Schulman, Filip Wolski, Prafulla Dhariwal, Alec Radford, and Oleg Klimov. Proximal policy optimization algorithms. *arXiv preprint arXiv:1707.06347*, 2017.

[49] Zhihong Shao, Peiyi Wang, Qihao Zhu, Runxin Xu, Junxiao Song, Xiao Bi, Haowei Zhang, Mingchuan Zhang, YK Li, Yang Wu, et al. Deepseekmath: Pushing the limits of mathematical reasoning in open language models. *arXiv preprint arXiv:2402.03300*, 2024.

[50] Charlie Victor Snell, Jaehoon Lee, Kelvin Xu, and Aviral Kumar. Scaling llm test-time compute optimally can be more effective than scaling parameters for reasoning. In *The Thirteenth International Conference on Learning Representations*, 2025.

[51] Chuanneng Sun, Songjun Huang, and Dario Pompili. Llm-based multi-agent reinforcement learning: Current and future directions. *arXiv preprint arXiv:2405.11106*, 2024.

[52] Kaiyang Wan, Lang Gao, Honglin Mu, Preslav Nakov, Yuxia Wang, and Xiuying Chen. A fano-style accuracy upper bound for llm single-pass reasoning in multi-hop qa. *arXiv preprint arXiv:2509.21199*, 2025.

[53] Peiyi Wang, Lei Li, Zhihong Shao, Runxin Xu, Damai Dai, Yifei Li, Deli Chen, Yu Wu, and Zhifang Sui. Math-shepherd: Verify and reinforce llms step-by-step without human annotations. In *Proceedings of the 62nd Annual Meeting of the Association for Computational Linguistics (Volume 1: Long Papers)*, pages 9426–9439, 2024.

[54] Xuezhi Wang, Jason Wei, Dale Schuurmans, Quoc Le, Ed Chi, Sharan Narang, Aakanksha Chowdhery, and Denny Zhou. Self-consistency improves chain of thought reasoning in language models. *arXiv preprint arXiv:2203.11171*, 2022.

[55] Jason Wei, Xuezhi Wang, Dale Schuurmans, Maarten Bosma, Fei Xia, Ed Chi, Quoc V Le, Denny Zhou, et al. Chain-of-thought prompting elicits reasoning in large language models. *Advances in neural information processing systems*, 35:24824–24837, 2022.

[56] Qingyun Wu, Gagan Bansal, Jieyu Zhang, Yiran Wu, Beibin Li, Erkang Zhu, Li Jiang, Xiaoyun Zhang, Shaokun Zhang, Jiale Liu, Ahmed Hassan Awadallah, Ryen W White, Doug Burger, and Chi Wang. Autogen: Enabling next-gen llm applications via multi-agent conversation, 2023. URL <https://arxiv.org/abs/2308.08155>.

[57] Shijie Xia, Yiwei Qin, Xuefeng Li, Yan Ma, Run-Ze Fan, Steffi Chern, Haoyang Zou, Fan Zhou, Xiangkun Hu, Jiahe Jin, et al. Generative ai act ii: Test time scaling drives cognition engineering. *arXiv preprint arXiv:2504.13828*, 2025.

[58] Yuxi Xie, Anirudh Goyal, Wenyue Zheng, Min-Yen Kan, Timothy P Lillicrap, Kenji Kawaguchi, and Michael Shieh. Monte carlo tree search boosts reasoning via iterative preference learning. *arXiv preprint arXiv:2405.00451*, 2024.

[59] Xiangyuan Xue, Yifan Zhou, Guibin Zhang, Zaibin Zhang, Yijiang Li, Chen Zhang, Zhenfei Yin, Philip Torr, Wanli Ouyang, and Lei Bai. Comas: Co-evolving multi-agent systems via interaction rewards. *arXiv preprint arXiv:2510.08529*, 2025.

- [60] An Yang, Anfeng Li, Baosong Yang, Beichen Zhang, Binyuan Hui, Bo Zheng, Bowen Yu, Chang Gao, Chengen Huang, Chenxu Lv, et al. Qwen3 technical report. *arXiv preprint arXiv:2505.09388*, 2025.
- [61] Feng Yao, Liyuan Liu, Dinghuai Zhang, Chengyu Dong, Jingbo Shang, and Jianfeng Gao. Your efficient rl framework secretly brings you off-policy rl training, august 2025. URL <https://fengyao.notion.site/off-policy-rl>, 2025.
- [62] Shunyu Yao, Dian Yu, Jeffrey Zhao, Izhak Shafran, Tom Griffiths, Yuan Cao, and Karthik Narasimhan. Tree of thoughts: Deliberate problem solving with large language models. *Advances in neural information processing systems*, 36:11809–11822, 2023.
- [63] Yao Yao, Zuchao Li, and Hai Zhao. Got: Effective graph-of-thought reasoning in language models. In *Findings of the Association for Computational Linguistics: NAACL 2024*, pages 2901–2921, 2024.
- [64] Qiying Yu, Zheng Zhang, Ruofei Zhu, Yufeng Yuan, Xiaochen Zuo, Yu Yue, Weinan Dai, Tiantian Fan, Gaohong Liu, Lingjun Liu, et al. Dapo: An open-source llm reinforcement learning system at scale. *arXiv preprint arXiv:2503.14476*, 2025.
- [65] Yufeng Yuan, Yu Yue, Ruofei Zhu, Tiantian Fan, and Lin Yan. What's behind ppo's collapse in long-cot? value optimization holds the secret. *arXiv preprint arXiv:2503.01491*, 2025.
- [66] Di Zhang, Xiaoshui Huang, Dongzhan Zhou, Yuqiang Li, and Wanli Ouyang. Accessing gpt-4 level mathematical olympiad solutions via monte carlo tree self-refine with llama-3 8b. *arXiv preprint arXiv:2406.07394*, 2024.
- [67] Guibin Zhang, Hejia Geng, Xiaohang Yu, Zhenfei Yin, Zaibin Zhang, Zelin Tan, Heng Zhou, Zhongzhi Li, Xiangyu Xue, Yijiang Li, et al. The landscape of agentic reinforcement learning for llms: A survey. *arXiv preprint arXiv:2509.02547*, 2025.
- [68] Kaiyan Zhang, Runze Liu, Xuekai Zhu, Kai Tian, Sihang Zeng, Guoli Jia, Yuchen Fan, Xingtai Lv, Yuxin Zuo, Che Jiang, Ziyang Liu, Jianyu Wang, Yuru Wang, Ruotong Zhao, Ermo Hua, Yibo Wang, Shijie Wang, Junqi Gao, Xinwei Long, Youbang Sun, Zhiyuan Ma, Ganqu Cui, Lei Bai, Ning Ding, Biqing Qi, and Bowen Zhou. Marti: A framework for multi-agent llm systems reinforced training and inference, 2025. URL <https://github.com/TsinghuaC3I/MARTI>.
- [69] Kechi Zhang, Ge Li, Jia Li, Yihong Dong, and Zhi Jin. Focused-dpo: Enhancing code generation through focused preference optimization on error-prone points. *arXiv preprint arXiv:2502.11475*, 2025.
- [70] Qiyuan Zhang, Fuyuan Lyu, Zexu Sun, Lei Wang, Weixu Zhang, Zhihan Guo, Yufei Wang, Irwin King, Xue Liu, and Chen Ma. What, how, where, and how well? a survey on test-time scaling in large language models. *CoRR*, 2025.
- [71] Qiyuan Zhang, Fuyuan Lyu, Zexu Sun, Lei Wang, Weixu Zhang, Wenyue Hua, Haolun Wu, Zhihan Guo, Yufei Wang, Niklas Muennighoff, et al. A survey on test-time scaling in large language models: What, how, where, and how well? *arXiv preprint arXiv:2503.24235*, 2025.
- [72] Yujie Zhao, Lanxiang Hu, Yang Wang, Minmin Hou, Hao Zhang, Ke Ding, and Jishen Zhao. Stronger-mas: Multi-agent reinforcement learning for collaborative llms. *arXiv preprint arXiv:2510.11062*, 2025.
- [73] Chujie Zheng, Shixuan Liu, Mingze Li, Xiong-Hui Chen, Bowen Yu, Chang Gao, Kai Dang, Yuqiong Liu, Rui Men, An Yang, et al. Group sequence policy optimization. *arXiv preprint arXiv:2507.18071*, 2025.
- [74] Andy Zhou, Kai Yan, Michal Shlapentokh-Rothman, Haohan Wang, and Yu-Xiong Wang. Language agent tree search unifies reasoning acting and planning in language models. *arXiv preprint arXiv:2310.04406*, 2023.
- [75] Sining Zhoubian, Dan Zhang, and Jie Tang. Rest-rl: Achieving accurate code reasoning of llms with optimized self-training and decoding. *arXiv preprint arXiv:2508.19576*, 2025.
- [76] Yuxin Zuo, Kaiyan Zhang, Li Sheng, Shang Qu, Ganqu Cui, Xuekai Zhu, Haozhan Li, Yuchen Zhang, Xinwei Long, Ermo Hua, et al. Ttrl: Test-time reinforcement learning. *arXiv preprint arXiv:2504.16084*, 2025.

Appendix

A Training Details

A.1 Training Infrastructure

Table 4: Training configurations and hyperparameters for Heter-MARS².

Category	Parameter
Model & Workflow Setup	
MCTS Nodes	16
Max Prompt Length	4096
Max Generation Length	32768
Eval Generation Length	32768
Max Sequence Length	40000
Overlong Buffer Length	2048
Cluster Configuration	
Reference Model Nodes	1 node \times 8 GPUs (per model)
Actor Nodes	1 node \times 8 GPUs (per model)
VLLM Engines	8 (per model)
Tensor Parallel Size	1
VLLM GPU Memory Utilization	0.85
Training Hyperparameters	
Training Batch Size	256
Micro Train Batch Size	1
Rollout Batch Size	512
Micro Rollout Batch Size	1
Number of Samples per Prompt	1
Learning Rate (Actor)	1e-6
Learning Rate (Critic)	9e-6
Initial KL Coefficient	1e-3
Gamma	1.0
KL Estimator	k3
Zero Stage	3
Precision	bfloat16
RL / PPO Settings	
Use KL Loss	Yes
Normalize Reward	Yes
Use Packing Samples	Yes
Dynamic Filtering Reward Range	[0, 1]
Dynamic Filtering for Agents	Enabled
IS Correction (vLLM)	Enabled
IS Truncated Threshold	2
Inference Settings	
Temperature	1.0
Top-p	1.0
Eval Temperature	1.0
Eval Samples per Prompt	1

B Detailed Experiments of MARS²

B.1 Heter-MARS² and Homo-MARS²

Table 5: Comparison of MARS²-T performance before and after training. For brevity, **DA-8B** denotes the combination of Qwen3-8B and AReaL-boba-2-8B, **DA-14B** denotes the combination of Qwen3-14B and AReaL-boba-2-14B, and **TA-14B** represents the three-model ensemble of Qwen3-14B, AReaL-boba-2-14B, and DeepCoder-14B-Preview.

single/multi agent	Pass@1	Pass@1(MCTS)			Pass@N budget=60
		budget=16	budget=37	budget=60	
Qwen-8B (w/o training)	50.3	56.0	56.6	54.3	68.6
Qwen-8B (w/ training)	55.4	56.6	56.6	60.6	71.4
AReaL-8B (w/o training)	51.0	54.9	54.9	56.0	66.9
AReaL-8B (w/ training)	55.4	57.7	59.4	58.3	69.7
DA-8B (w/o training)	50.3/51.4	56.0	55.4	57.2	69.7
DA-8B (w/ training)	58.3/54.9	64.0	61.7	61.7	75.4
Qwen-14B (w/o training)	56.0	61.1	61.7	63.4	75.4
Qwen-14B (w/ training)	61.1	64.0	66.3	65.1	78.9
AReaL-14B (w/o training)	58.4	61.1	65.7	64.6	74.3
AReaL-14B (w/ training)	62.3	66.3	72.6	68.0	81.1
DeepCoder-14B (w/o training)	50.8	56.0	57.1	57.1	67.4
DeepCoder-14B (w/ training)	54.3	58.3	56.6	60.6	70.9
DA-14B (w/o training)	56.0/58.4	61.7	60.0	62.9	74.9
DA-14B (w/ training)	61.7/64.6	67.7	68.0	68.9	79.4
TA-14B (w/o training)	56.0/58.4/50.8	61.1	62.3	61.1	76.6
TA-14B (w/ training)	56.6/64/52	68.0	65.7	66.9	80.0

B.2 Test-time Search Efficiency

We conduct a comprehensive evaluation of MARS²-T+ to validate its search efficiency and scalability before training.

- **System Performance.** We evaluate MARS²-T+ algorithm by comparing its performance with LLM-based single-agent’s initial performance as well as with standard Best-of-N algorithm. Empirical results in Table 6 indicate that MARS²-T+ algorithm achieves consistently superior performance. These results collectively demonstrate the efficiency of the MARS²-T+ algorithm.
- **Scaling Trend (Compute & Agents).** We identify scaling trends across two dimensions. Regarding generation budgets, performance improves steadily as more budget is allocated, systematically capitalizing on additional computational resources until stabilizing at a budget of XX. Regarding agent scaling, multi-agent MCTS consistently outperforms the strongest single-agent setup. The performance continues to improve as the number of agents increases, beyond which the system saturates. This highlights the effectiveness of multi-agent collaboration in enhancing exploration efficiency.
- **Ablation Studies.** We validate the impact of reward model and error message. The integration of reward model for node selection consistently outperforms the baseline strategy that selects nodes in reverse generation order, proving its effectiveness in prioritizing high-quality reasoning trajectories. Furthermore, augmenting MARS²-T+ with error message feedback yields superior results compared to the version without feedback, indicating that leveraging error signals can steer search and enhance overall performance.

Table 6: **Performance of single-agent and multi-agent test-time scaling.** Q-8B denotes Qwen3-8B; A-8B denotes AReal-boba-2-8B; DS-Q-8B denotes DeepSeek-R1-0528-Qwen3-8B; DS-L-8B denotes DeepSeek-R1-Distill-Llama-8B; Q-14B denotes Qwen3-14B; A-14B denotes AReal-boba-2-14B; DC-14B denotes Deepcoder-14B-preview ; DS-Q-14B denotes DeepSeek-R1-Distill-Qwen-14B.

single/multi agent	initial performance	Best of N (Pass@1) N=150	System Performance (Pass@1)			System Performance (Pass@K) budget=150
			budget=60	budget=100	budget=150	
Q-8B	0.503	0.554	0.543	0.576	0.570	0.703
A-8B	0.510	0.526	0.560	0.556	0.538	0.675
DA-8B	-	-	0.572	0.543	0.560	0.714
Q-14B	0.560	0.600	0.634	0.636	0.630	0.766
A-14B	0.584	0.594	0.646	0.652	0.674	0.760
DC-14B	0.508	0.514	0.571	0.539	0.536	0.737
DS-Q-14B	0.530	0.566	0.571	0.571	0.571	0.680
DA-14B	-	-	0.629	0.623	0.646	0.760
TA-14B	-	-	0.611	0.608	0.615	0.771
QA-14B	-	-	0.623	0.657	0.628	0.789

B.3 The Limitations of AB-MCTS

Insufficient error utilization. AB-MCTS treats failed nodes as providing only binary feedback (e.g., pass/-fail), which limits the model’s ability to learn from mistakes. Consequently, it fails to exploit richer diagnostic signals—such as input–output mismatches or runtime error traces—that could otherwise guide more effective iterative refinement. We provide the original refinement prompt template used in AB-MCTS to illustrate this limitation. The template for our enhanced error-feedback mechanism is presented in Appendix C.1.

Limited depth for refinement. The algorithm tends to generate wide but shallow trees, which severely impedes the deep iterative refinement required to solve complex code generation problems. We evaluate AB-MCTS and its multi-agent variants on the LiveCodeBench-v6 benchmark, using 175 tasks with 100 node expansions per task. As detailed in Table 7, AB-MCTS exhibits a strong bias toward shallow exploration: over 95% of nodes are concentrated within the first three levels. This tendency becomes even more pronounced in multi-agent settings, indicating that the algorithm does not fully exploit the collaborative advantages necessary for solving complex tasks.

Table 7: Node depth distribution (%) on LiveCodeBench-v6 with 175 tasks (100 node expansions per task). Most nodes lie within the first three levels, indicating shallow exploration behavior. **Q**, **A**, and **D** denote *Qwen3-8B*, *Areal-8B*, and *DeepSeek-R1-0528-Qwen3-8B*, respectively. **Q+A** and **Q+A+D** represent 2-agent and 3-agent configurations.

Model	1st layer	2nd layer	3rd layer	4th layer	≥ 5 th layer
Qwen3-8B	46.51	36.38	13.23	3.29	0.51
Areal-8B	41.14	42.30	13.54	2.50	0.52
DeepSeek-R1-0528-Qwen3-8B	54.19	32.15	11.42	2.02	0.22
2 model(Q+A)	45.33	40.23	12.56	1.69	0.19
3 model(Q+A+D)	66.59	28.74	4.31	0.33	0.03

To further control for task difficulty, we analyze a subset containing only *hard-level* samples. The depth distribution (Table 8) reveals a similar pattern: despite a slight shift toward deeper exploration, most nodes still cluster in the first three layers, especially in multi-agent variants.

This shallow search behavior suggests that AB-MCTS has not fully exploited the potential of multi-agent collaboration, thereby limiting its ability to achieve deeper iterative refinement on challenging code generation tasks.

Table 8: Node depth distribution (%) on the hard subset of LiveCodeBench-v6. The shallow-search tendency remains evident in multi-agent variants.

Model	1st layer	2nd layer	3rd layer	4th layer	≥ 5 th layer
Qwen3-8B	35.43	38.84	19.03	5.66	1.05
Areal-8B	31.96	47.05	16.58	3.50	0.91
DeepSeek-R1-0528-Qwen3-8B	38.83	40.61	17.00	3.16	0.40
2 model(Q+A)	35.51	43.55	17.90	2.74	0.30
3 model(Q+A+D)	62.53	31.88	5.15	0.40	0.05

B.4 Prompt of MARS²-T+

Vanilla-TTS Prompt

You are an expert Python programmer. You will be given a question (problem specification) and will generate a correct Python program that matches the specification and passes all tests. Here's your last question and your answer:

Question:{}

Your previous code:{}

Result: Wrong

Summary

Your solution is correct for 0 problems among 1, please re-implement your code. In addition to passing the test cases, try to ensure that your code can handle various input cases as much as possible, including edge cases and exceptions.

Answer: (use the provided format with backticks)

C Reward Model Details

C.1 Training Data Construction

Data Source and Generation. We utilize the DeepCoder dataset as the problem pool. For each problem x , we employ a simple parallel sampling method. Specifically, we use each policy model \mathcal{A}_j from our pool (e.g., Qwen3-8B, areal-boba-2-8B, etc.) to independently generate $N = 8$ candidate solutions y for the same prompt.

The collected nodes from all models are then aggregated.

Ground-Truth Labeling. Each generated solution y is executed against the problem's private test cases to obtain the ground-truth environment reward $r \in \{0, 1\}$, where $r = 1$ signifies passing all test cases and $r = 0$ otherwise.

Data Formatting. From this labeled corpus, we derive two distinct training formats, which correspond to two complementary training objectives:

MARS²-T+Prompt

You are an expert Python programmer. You will be given a question (problem specification) and will generate a correct Python program that matches the specification and passes all tests. Here's your last question and your answer:

Question:

Format: Read the inputs from `stdin` solve the problem and write the answer to `stdout` (do not directly test on the sample inputs). Enclose your code within delimiters as follows. Ensure that when the python program runs, it reads the inputs, runs the algorithm and writes output to `STDOUT`.

`'''python`

`YOUR CODE HERE`

`'''`

Your previous code:

Next, please re-implement your code. In addition to passing the test cases, try to ensure that your code can handle various input cases as much as possible, including edge cases and exceptions.

TASK: Deep Code Repair and Generalization

Here is the test report from the last execution:

Execution Summary: - Passed out of test cases (pass rate).

Detailed Failure Analysis:

— Failure on Test Case 1 —

Reason: Wrong Answer

Input:

Your code's output:

Expected output:

WARNING: Do not write special-case code (e.g., using an "if" statement for a specific input) just to fix the failures listed above. This "patching" approach will fail on unseen test cases.

Your Goal: Treat the failed cases as clues to find and fix the fundamental algorithmic or logical flaw in the code.

Please follow this thinking framework to provide a generalized solution:

1. Pattern Analysis:

Examine all failed test cases. Are they edge cases (e.g., empty lists, zero, max values)? Data type issues (e.g., integer vs. float)? Or inputs with a specific pattern?

Compare successful vs. failed cases and ask: "Under what conditions does my algorithm break?"

2. Root Cause Deduction:

Based on the pattern, pinpoint the specific defect in the code. Is it a wrong loop condition? Improper variable initialization? A missing base case in recursion? Or a flaw in the overall algorithm logic?

3. General Fix Strategy:

Formulate a plan that corrects the root cause. This fix must naturally pass all known failed cases and generalize to similar, unseen ones.

4. Provide Final Code:

Based on your general fix strategy, provide the complete and immediately runnable corrected code.

Do not add any explanations, comments, or dialogue before or after the code.

Answer: (use the provided format with backticks)

- **Pointwise Data:** Each tuple is formatted as (x, y, r) . This data is used to train the RM to predict the absolute correctness (i.e., pass probability) of a solution.
- **Pairwise Data:** We generate preference pairs (x, y_w, y_l) , where y_w ("winner") is a preferred solution over y_l ("loser"). These pairs are primarily constructed by sampling solutions with different ground-truth rewards (e.g., $r(y_w) = 1$ and $r(y_l) = 0$) for the same problem x . This format is crucial for training the model on relative ranking.

C.2 Training Objectives

We initialize our RM R_θ from the Skywork-Reward-V2-Qwen3-8B checkpoint. The model takes (x, y) as input and outputs a scalar score $s = R_\theta(x, y)$. We train this model using two complementary objectives:

Mean Squared Error (MSE) Loss. As defined in the main paper (Equation 6), this objective trains the RM as a fine-grained predictor of pass probability. We apply a sigmoid function $\sigma(\cdot)$ to the output score and optimize against the binary ground-truth label r :

$$L_{MSE} = (\sigma(R_\theta(x, y)) - r)^2 \quad (17)$$

Bradley-Terry (BT) Pairwise Loss. To explicitly train the RM on relative preferences, we utilize the Bradley-Terry model. For a given preference pair (x, y_w, y_l) , the loss function encourages the score of the winning solution y_w to be higher than that of the losing solution y_l :

$$L_{BT} = -\log(\sigma(R_\theta(x, y_w) - R_\theta(x, y_l))) \quad (18)$$

In our experiments, we compare the performance of RMs trained with L_{MSE} versus those trained with L_{BT} on our benchmark.

C.3 Benchmark Construction for RM Evaluation

Benchmark Source. The benchmarks are derived from tasks in `livecodebench_v6` (175 tasks), which are entirely separate from our DeepCoder-based training data.

Generation Process. To generate the dataset, we employed two distinct groups of reasoning models, categorized by parameter size. The first group consists of 14B-parameter models: `Qwen3-14B`, `areal-boba-2-14B`, and `deepcoder-14B-preview`. The second group comprises 8B-parameter models: `Qwen3-8B` and `areal-boba-2-8B`. We utilized these models to run AB-MCTS on the held-out tasks, collecting a diverse set of solutions and their corresponding ground-truth outcomes.

Benchmark Instances. We constructed two distinct sets of benchmarks to evaluate performance across different training stages. Both sets encompass solutions generated by the 8B and 14B model groups. For these extracted benchmarks, we specifically ensured a balanced distribution between data with a score of 1 and a score of 0.

- **Pre-train Benchmark (150 nodes):** Constructed using solutions generated by the models prior to training. This dataset collects the top 150 nodes per task.
- **Post-train Benchmark (60 nodes):** Created using solutions generated by the models after training. This dataset collects the top 60 nodes per task.

Evaluation Metrics Definition. To comprehensively evaluate the Reward Model’s ranking capability and robustness against score distribution shifts, we employ three key metrics on the pointwise benchmark data:

- **AUC-ROC:** The Area Under the Receiver Operating Characteristic curve. This metric evaluates the model’s ability to rank positive samples higher than negative ones across all possible decision thresholds, serving as a calibration-independent measure of discriminative power.
- **Spearman Correlation:** The rank-order correlation coefficient between the predicted reward scores and the ground truth labels. It assesses the monotonicity of the predictions, ensuring that better responses consistently receive higher scores regardless of the absolute value range.
- **Adaptive Accuracy:** The binary classification accuracy calculated using the median of the predicted logits as the dynamic decision threshold (instead of a fixed threshold like 0 or 0.5). This metric mitigates the impact of uncalibrated score distributions (e.g., negative bias) and focuses on the model’s intrinsic ability to separate positive and negative samples.

D Diversity Analysis of Our TTS-Enhanced Method

In Section 5.2, we primarily analyzed the diversity metrics of the MARS² training method. In this section, we evaluate the diversity performance of our proposed TTS-enhanced method.

We extend the node budget from 60 to 100 to better demonstrate the potential of the approach. We select 104 tasks that can be successfully completed by both AB-MCTS and the MARS² method (see Section 3.3.1) and compute their diversity metrics. The results are visualized in Figure 13.

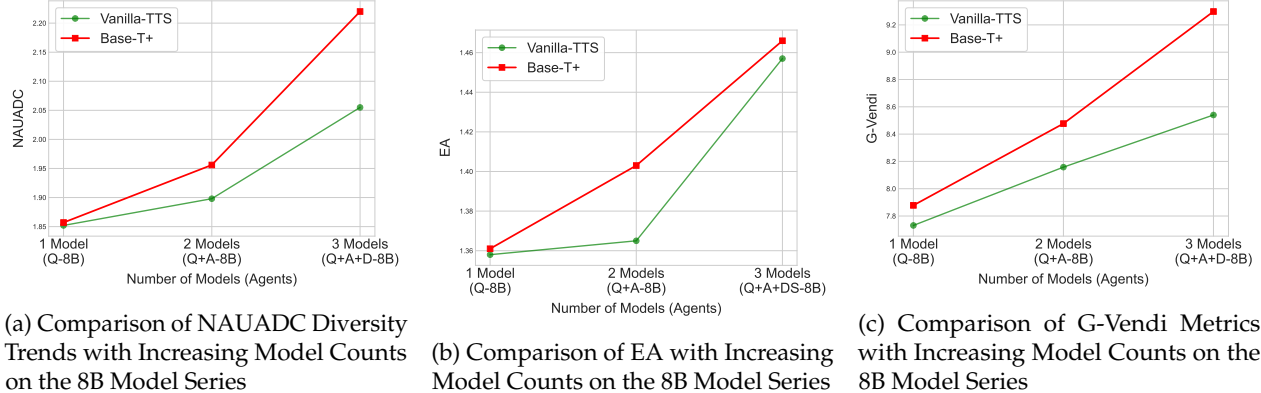


Figure 13: Analysis of Diversity metrics Trends with Increasing Model Counts across 8B and 14B Model Series.

As the number of models increases, the NAUADC, EA, and G-Vendi metrics all improve, further corroborating our main conclusion: **algorithmic diversity and distributional uniformity increase with the number of models**. Moreover, our proposed TTS-enhanced method, MARS², consistently outperforms AB-MCTS across all diversity metrics, particularly in multi-model settings. This demonstrates that MARS² effectively enhances algorithmic diversity, distributional uniformity, and strategic diversity.

To further investigate the mechanism by which our method enhances diversity, we categorize tasks by difficulty into 43 easy, 35 medium, and 26 hard tasks. We compute diversity metrics for the 8B-class models on each category separately, with results shown in Table 9.

Table 9: Detailed diversity metric statistics for 8B series models.

Method	Pass@K	AEC			DA@K			EA			NAUADC			G-Vendi			
		E.	M.	H.	E.	M.	H.	E.	M.	H.	E.	M.	H.	E.	M.	H.	
AB-MCTS																	
Q-8B		0.725	1.09	1.09	1.00	1.30	1.50	1.71	1.23	1.39	1.53	1.50	1.95	2.31	8.67	7.60	6.34
A-8B		0.691	1.09	1.06	1.00	1.19	1.60	1.72	1.14	1.44	1.54	1.33	2.07	2.29	9.39	7.50	5.96
Q-8B+A-8B		0.737	1.23	1.40	1.50	1.32	1.55	1.76	1.24	1.38	1.55	1.58	2.07	2.19	9.43	8.07	6.17
Q-8B+A-8B+DS-8B		0.697	1.47	1.94	1.96	1.44	1.58	1.91	1.33	1.45	1.68	1.74	2.12	2.48	12.20	6.93	4.66
MARS²																	
Q-8B		0.742	1.14	1.09	1.19	1.33	1.51	1.73	1.24	1.36	1.57	1.51	1.96	2.29	8.78	7.66	6.67
Q-8B+A-8B		0.754	1.07	1.09	1.23	1.30	1.61	1.83	1.22	1.45	1.64	1.52	2.09	2.50	10.05	7.99	6.54
Q-8B+A-8B+DS-8B		0.737	1.21	1.77	1.92	1.37	1.67	2.05	1.27	1.48	1.77	1.72	2.37	2.84	12.79	7.89	5.42

Based on this table, we obtain several intriguing findings.

MARS² significantly enhances algorithmic diversity on high-difficulty tasks. Compared to AB-MCTS, the MARS² method achieves consistently higher scores on diversity metrics such as DA@K, EA, and NAUADC, with the improvement most pronounced on medium and hard tasks. For instance, under the three-model ensemble setting (Q+A+DS), MARS² attains a NAUADC score of 2.84 on hard tasks, substantially outperforming AB-MCTS's score of 2.48. This indicates that MARS²'s multi-agent collaboration mechanism effectively promotes divergent reasoning when tackling complex problems, helping to avoid convergence to a single erroneous trajectory.

Strategic diversity (G-Vendi) exhibits a clear decreasing trend of “Easy > Medium > Hard”. Across both single-model and multi-model settings, the G-Vendi score consistently declines as task difficulty increases. This pattern likely arises because easy tasks permit models to generate richer and more divergent chains of thought—multiple distinct reasoning pathways can lead to the correct answer. In contrast, hard tasks impose stringent logical constraints, narrowing the solution space and thereby reducing the heterogeneity of viable reasoning trajectories.

Cumulative diversity gains from heterogeneous model integration. Comparing the results of single-model (Q-8B), two-model (Q+A), and three-model (Q+A+DS) setups reveals a steady improvement in all diversity metrics (particularly AEC and NAUADC) as more heterogeneous models are integrated. notably, while the three-model ensemble under MARS² achieves the highest diversity scores (e.g., a G-Vendi of 12.79 on Easy tasks), its Pass@K (0.737) is slightly lower than that of the two-model ensemble (0.754). This indicates that extreme diversity does not always translate linearly into accuracy improvements; in some cases, introducing highly divergent models may introduce noise, highlighting the need to balance diversity and precision.